US006528208B1

(12) **United States Patent**
Thackeray et al.

(10) **Patent No.:** **US 6,528,208 B1**
(45) **Date of Patent:** **Mar. 4, 2003**

(54) **ANODES FOR RECHARGEABLE LITHIUM BATTERIES**

(75) Inventors: **Michael M. Thackeray**, Naperville, IL (US); **Keith D. Kepler**, Mountain View, CA (US); **John T. Vaughey**, Elmhurst, IL (US)

(73) Assignee: **The University of Chicago**, Chicago, IL (US)

(*) Notice: Subject to any disclaimer, the term of this patent is extended or adjusted under 35 U.S.C. 154(b) by 0 days.

(21) Appl. No.: **09/622,617**

(22) PCT Filed: **Oct. 15, 1999**

(86) PCT No.: **PCT/US99/24168**

§ 371 (c)(1),
(2), (4) Date: **Oct. 26, 2000**

(87) PCT Pub. No.: **WO00/38258**

PCT Pub. Date: **Jun. 29, 2000**

Related U.S. Application Data

(60) Provisional application No. 60/092,206, filed on Jul. 9, 1998, and provisional application No. 60/142,312, filed on Dec. 21, 1998.

(51) **Int. Cl.^{7}** **H01M 4/38**

(52) **U.S. Cl.** **429/218.1**; 429/231.95
(58) **Field of Search** 252/182.1; 429/218.1, 429/231.1, 231.95

(56) **References Cited**

U.S. PATENT DOCUMENTS

5,770,333 A * 6/1998 Saito et al. 252/182.1
6,203,944 B1 * 3/2001 Turner et al. 252/182.1

OTHER PUBLICATIONS

Yang et al., Solid State Ionics, 90 (1996) pp. 281–287.*
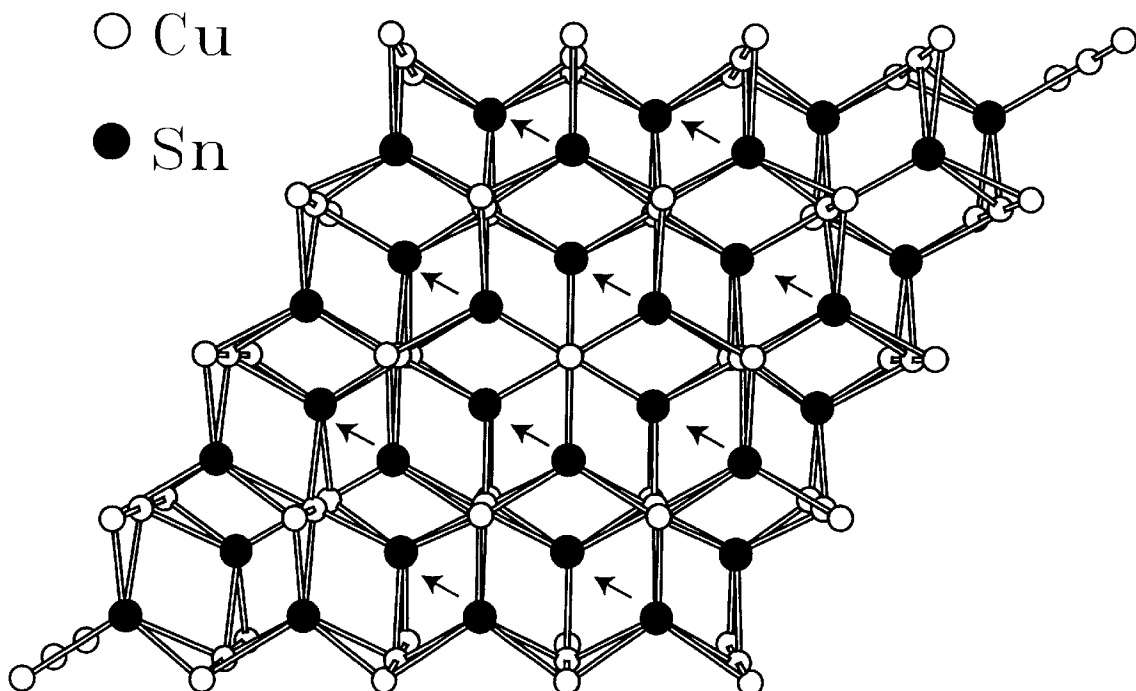
* cited by examiner

Primary Examiner—Carol Chaney
(74) *Attorney, Agent, or Firm*—Emrich & Dithmar

(57) **ABSTRACT**

A negative electrode (12) for a non-aqueous electrochemical cell (10) with an intermetallic host structure containing two or more elements selected from the metal elements and silicon, capable of accommodating lithium within its crystallographic host structure such that when the host structure is lithiated it transforms to a lithiated zinc-blende-type structure. Both active elements (alloying with lithium) and inactive elements (non-alloying with lithium) are disclosed. Electrochemical cells and batteries as well as methods of making the negative electrode are disclosed.
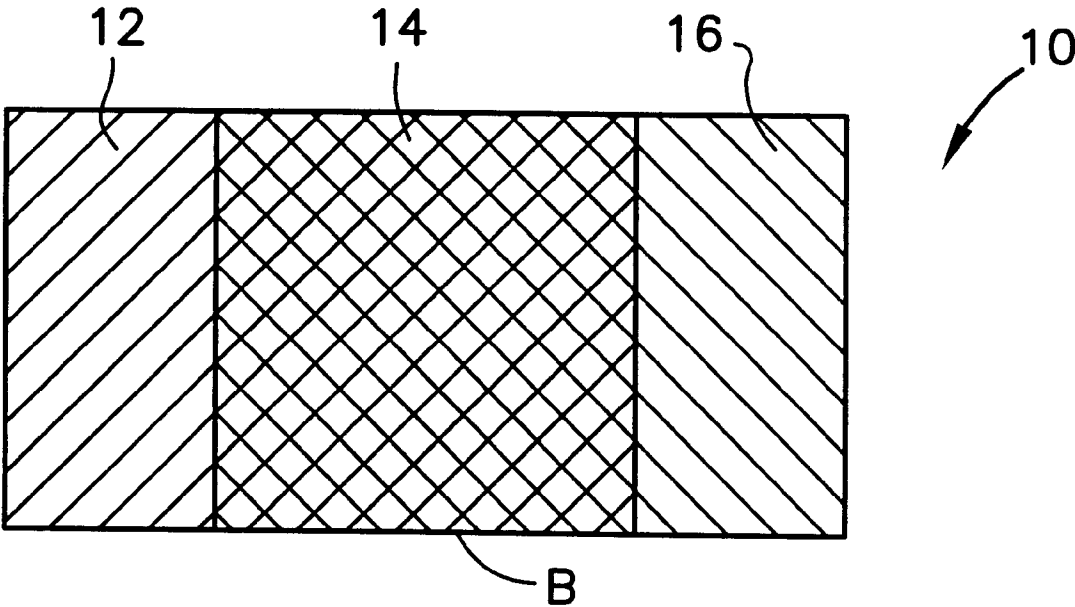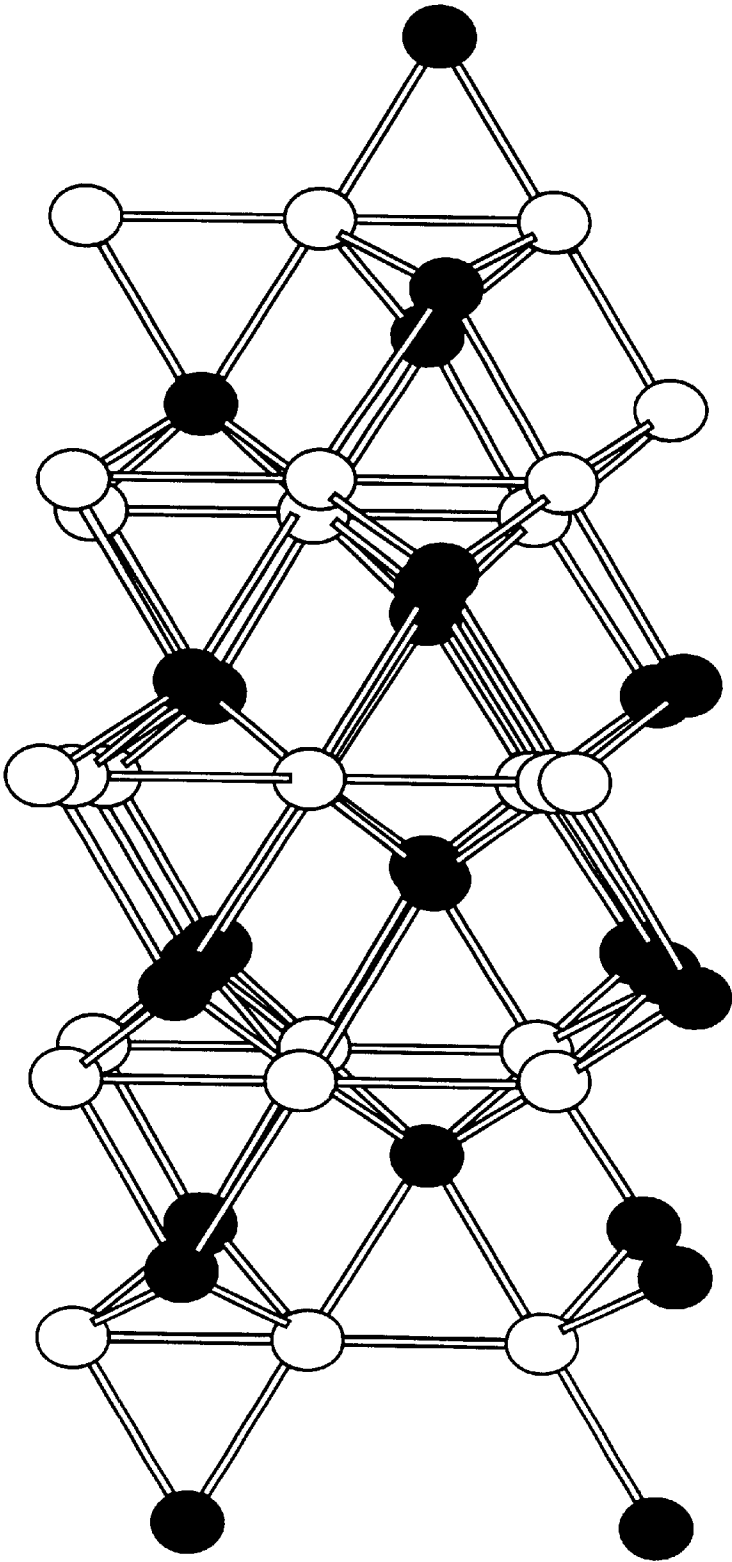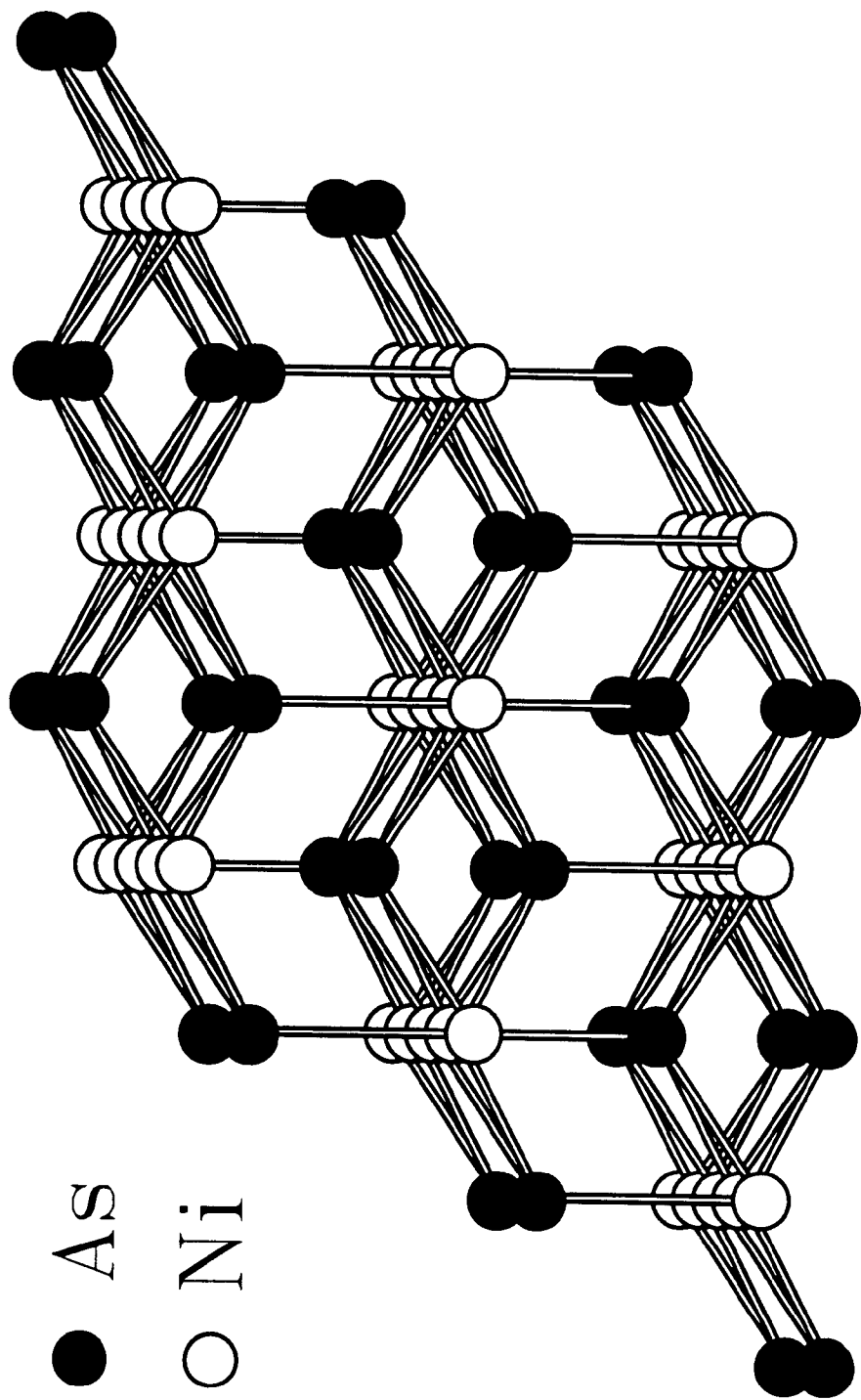
41 Claims, 29 Drawing Sheets

FIG. 1
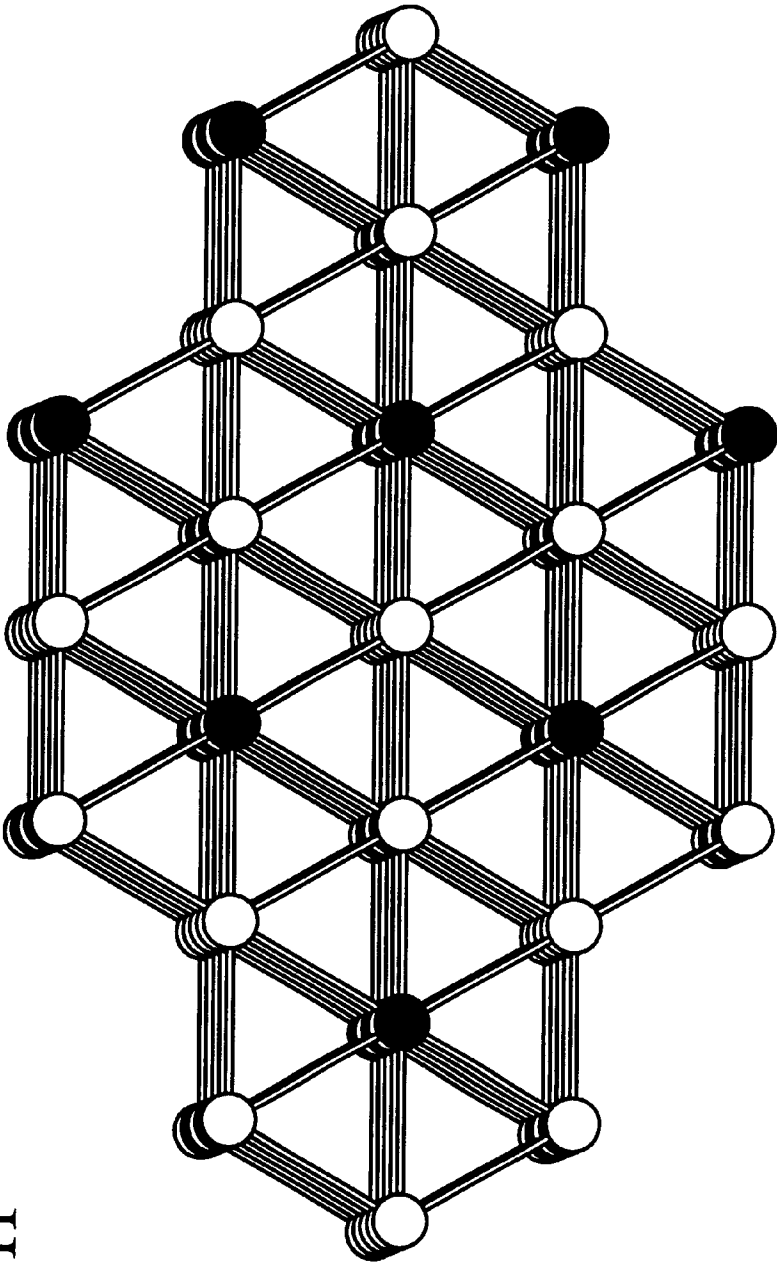
FIG. 2

○ Cu
● Sn

FIG. 3

FIG. 4

○ Ni

● In

○ Cu

● Sn

FIG. 5a

FIG. 5b

Sn ●
Cu ○
Cu-i ●

FIG. 6

○ Ni/Co

● Sn

2-Theta

FIG. 7

FIG. 8a

Li

Cu

Sn

FIG. 8b

Sn

Li,Cu

Li

FIG. 8c

Cu Sn

FIG. 9

○ Li
● Cu
○ Sn
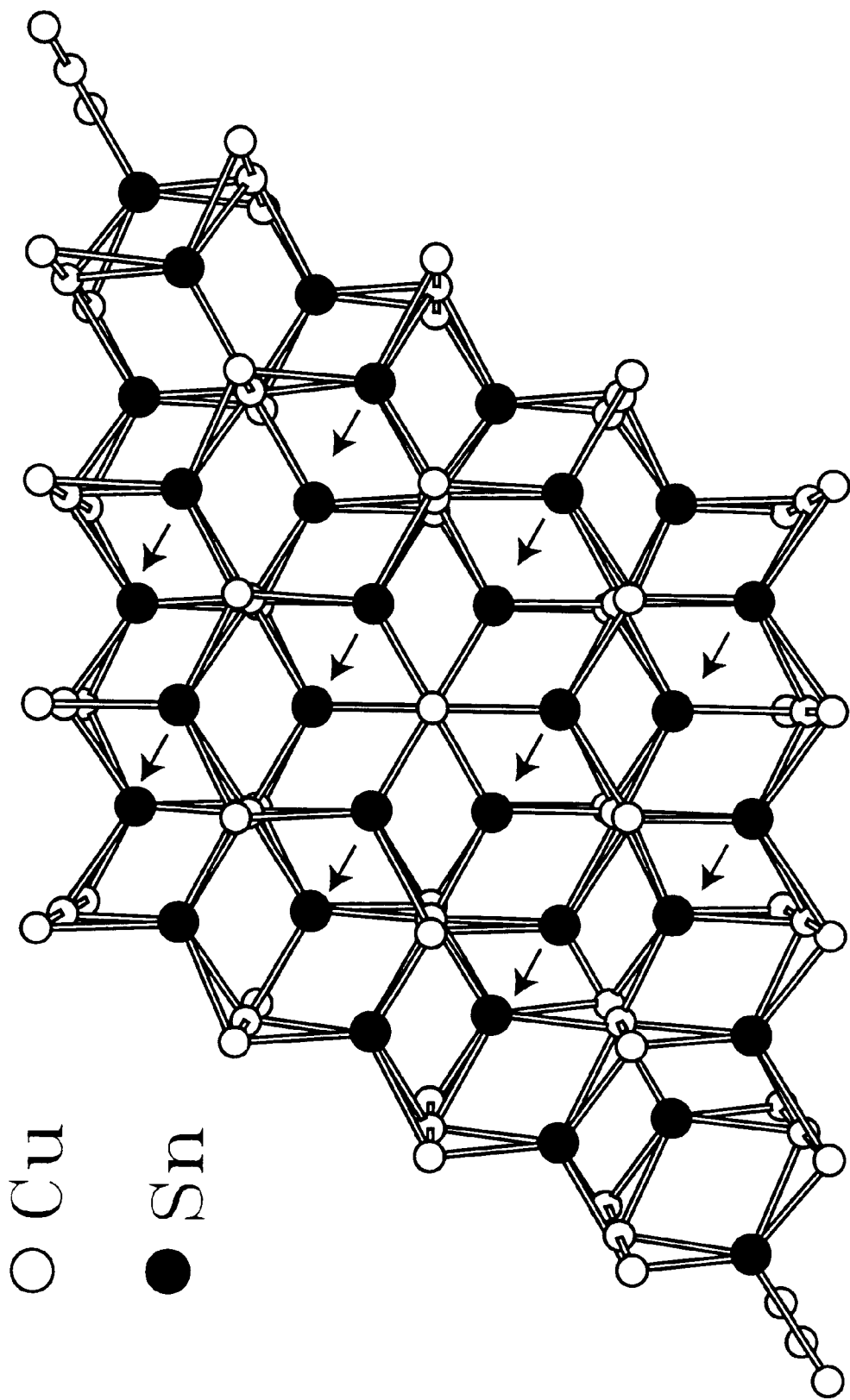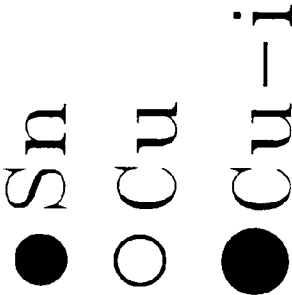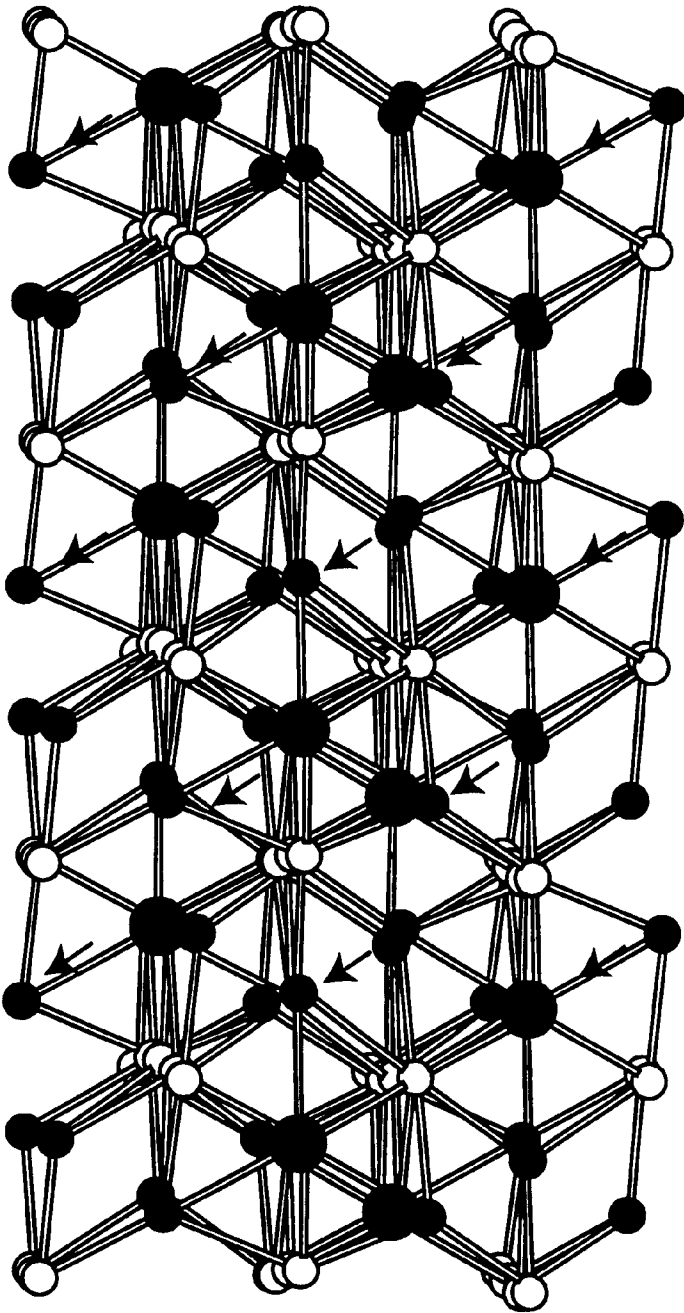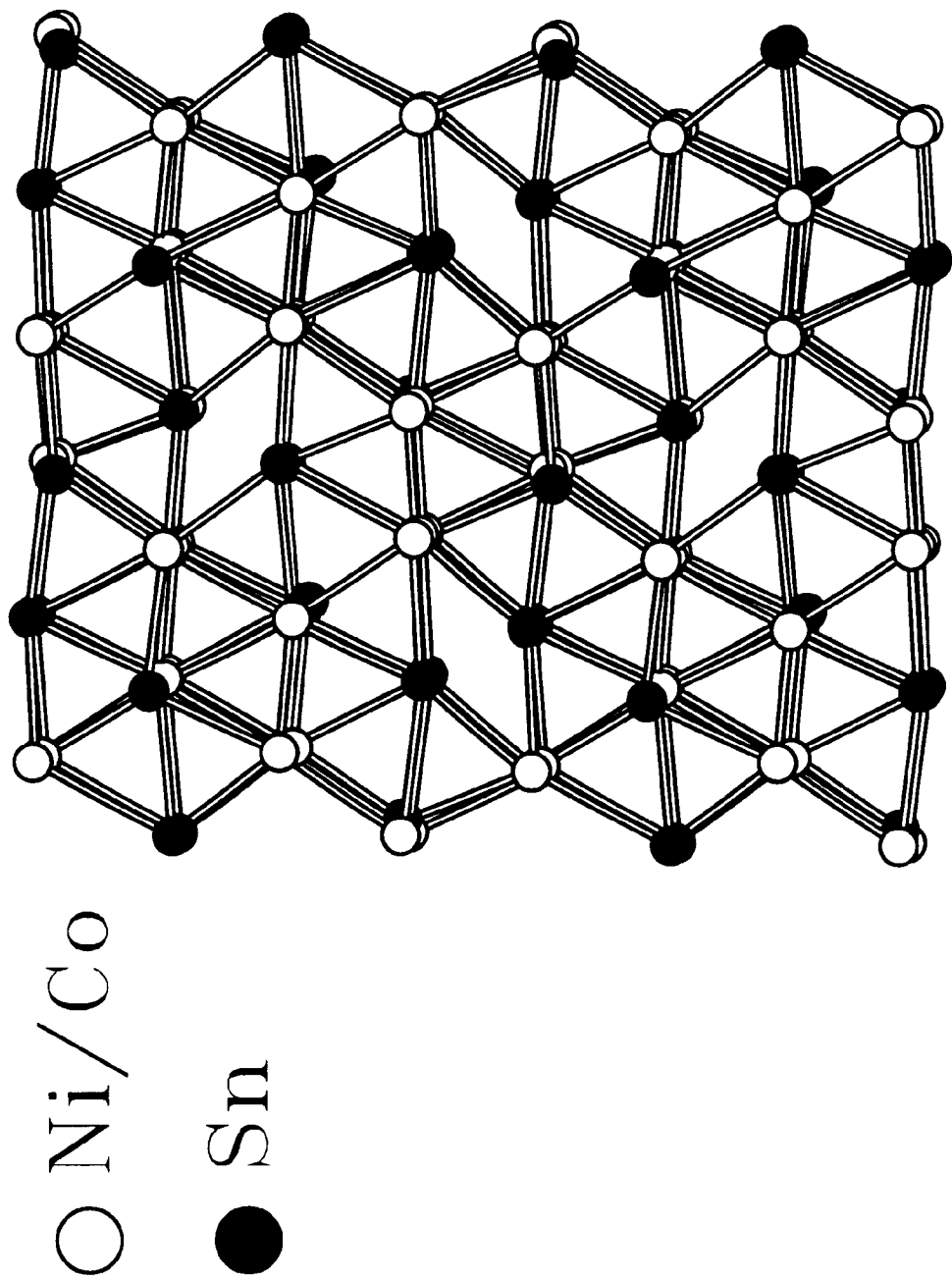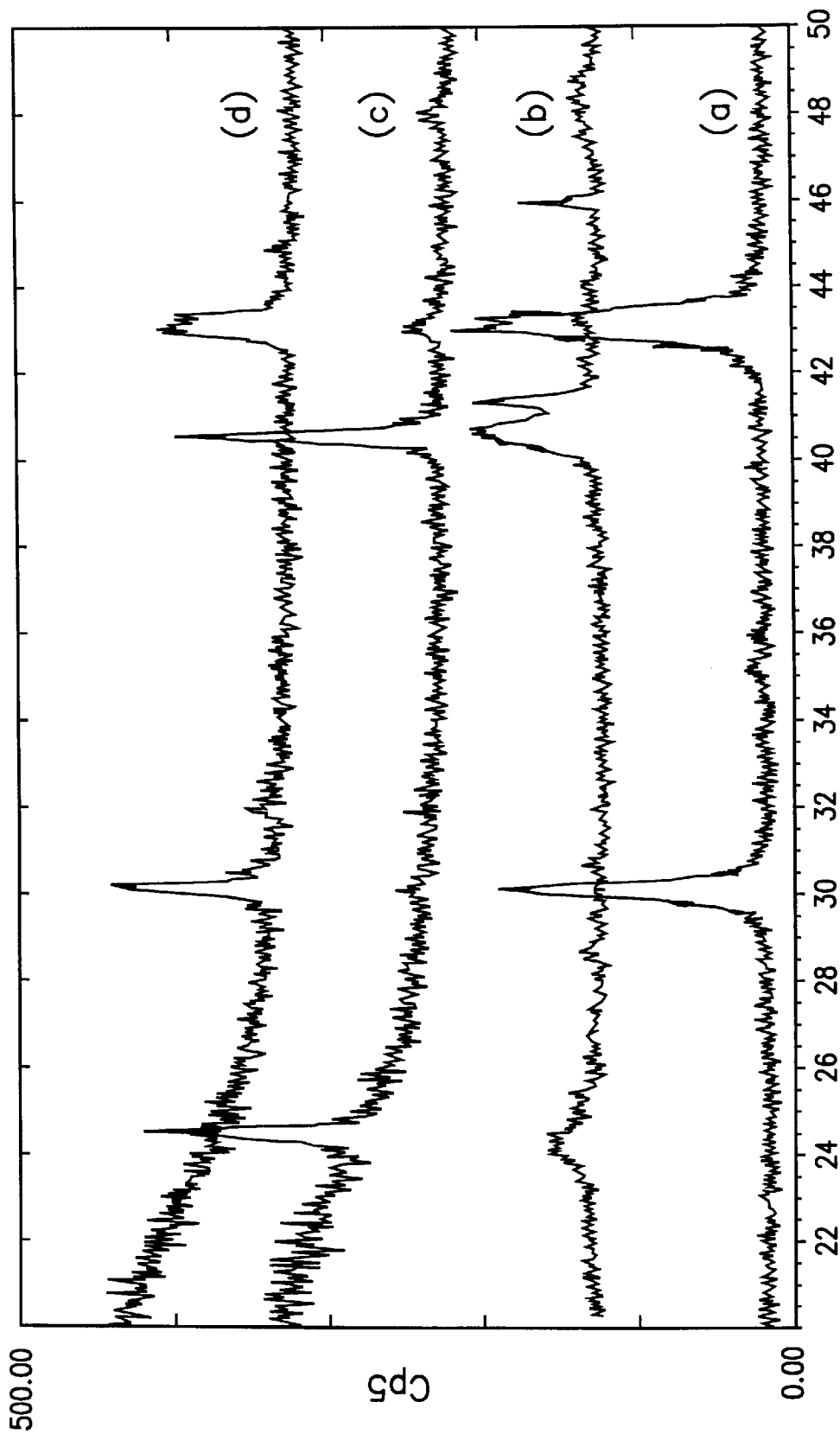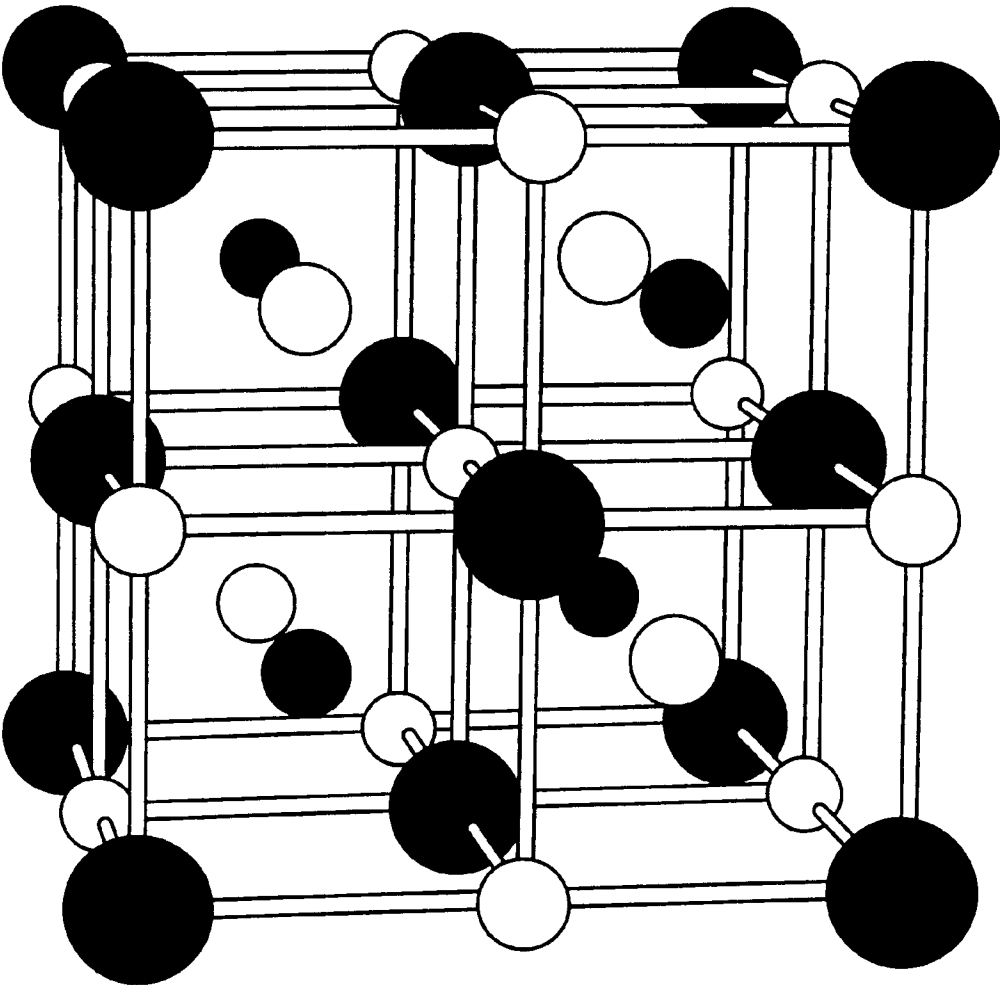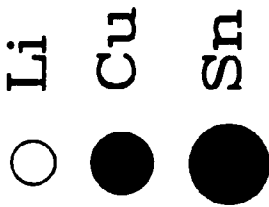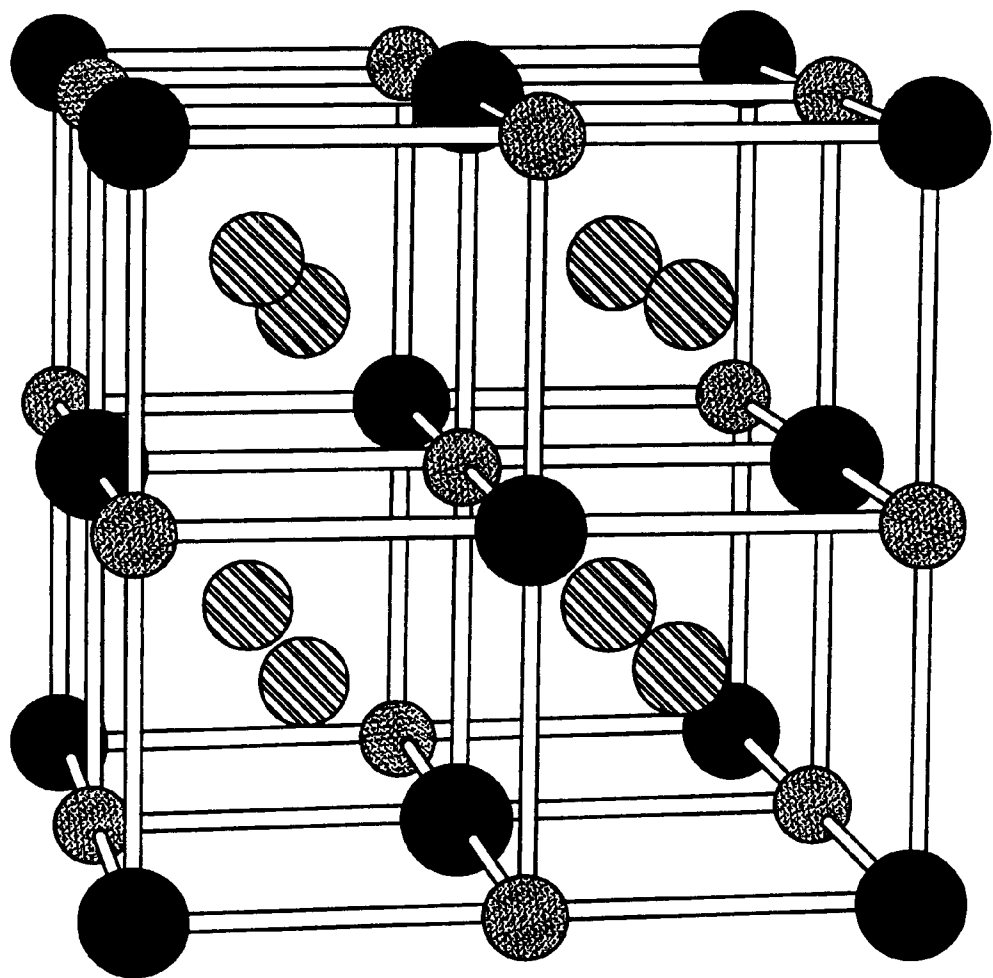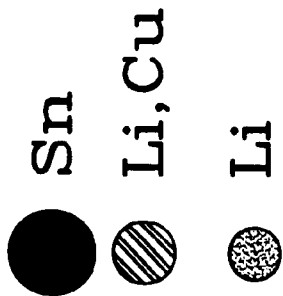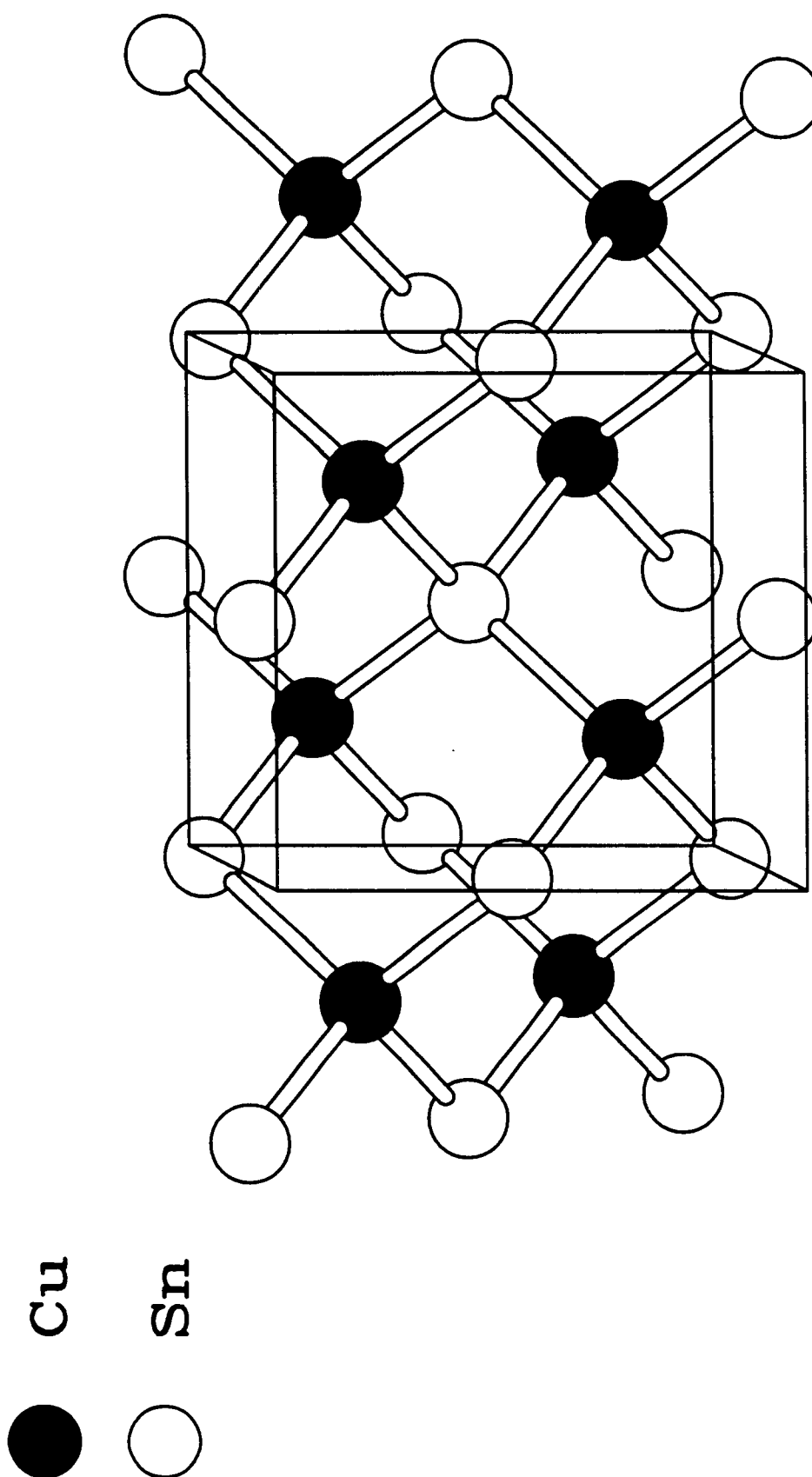
FIG. 10

FIG. 11

FIG. 12

FIG. 13

FIG. 14

FIG. 15

(VOLTAGE RANAGE 1.2 TO 0 V)

■ Sn
× Cu6Sn6
▲ Cu6Sn5
△ Cu6Sn5,Ball Milled 10 hrs
□ Cu6Sn5,Ball Milled 10 hrs
◆ Cu6Sn4
◁ Cu6Sn4,Ball Milled 5 hrs
◇ Cu6Sn2,Ball Milled 5 hrs
● Li2CuSn

CELL CAPACITY (mAh/g)

CYCLE NUMBER

FIG. 16

Sn–Cu Alloys as Anodes, 1.2 V – 0.2 V

FIG. 17

FIG. 18

FIG. 19

FIG. 20

* CURRENT COLLECTOR PEAKS
o SAMPLE HOLDER
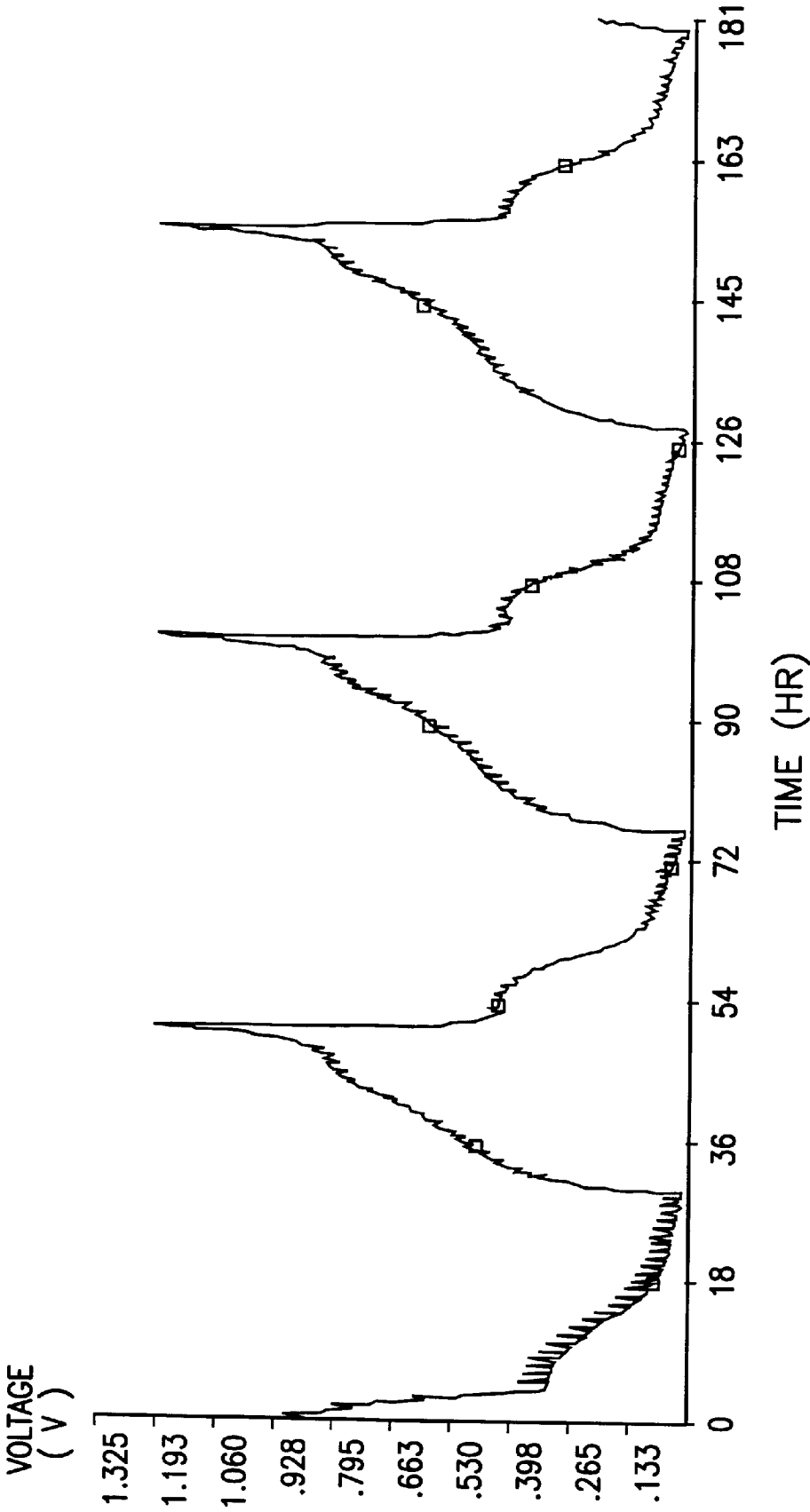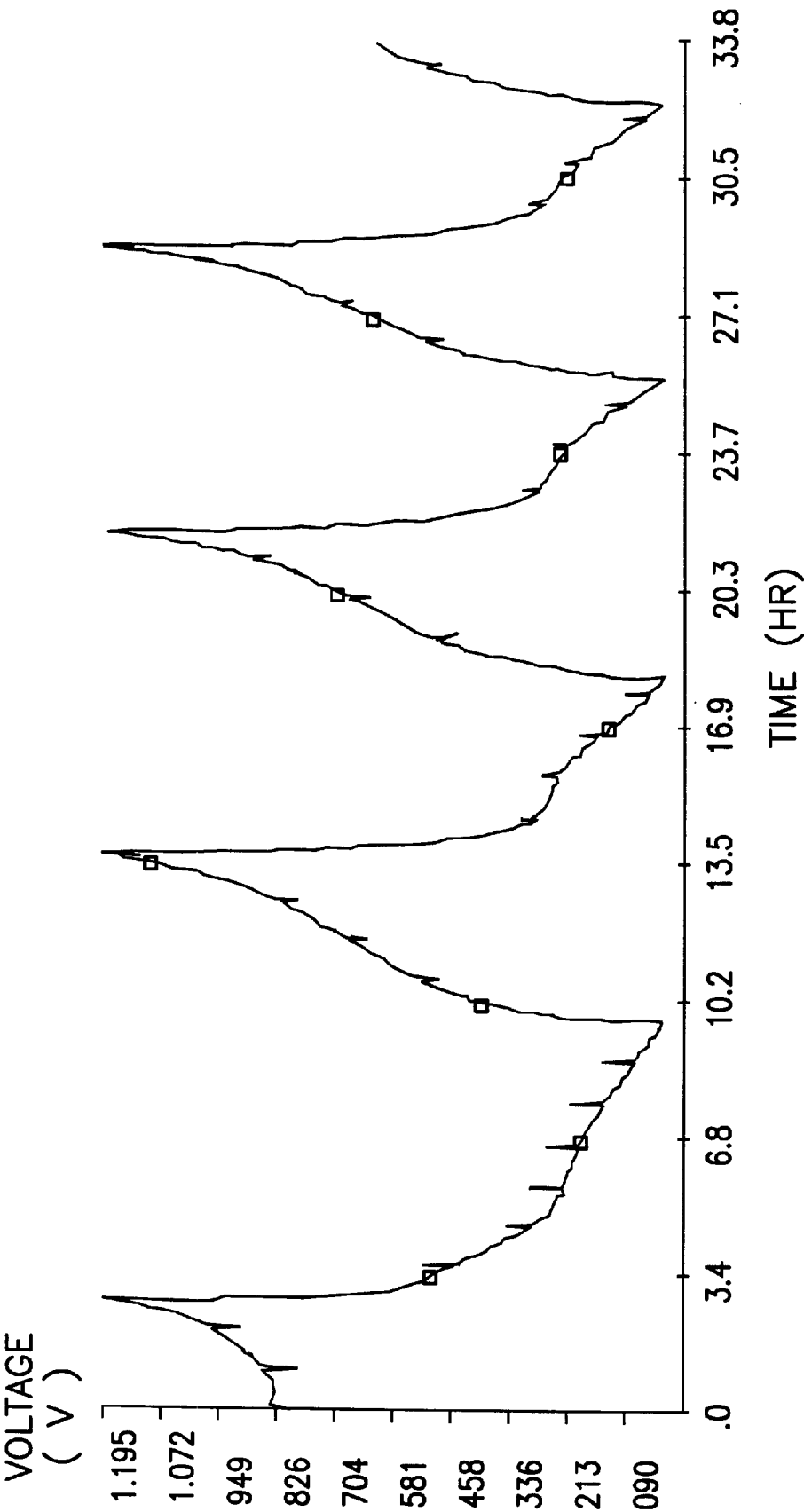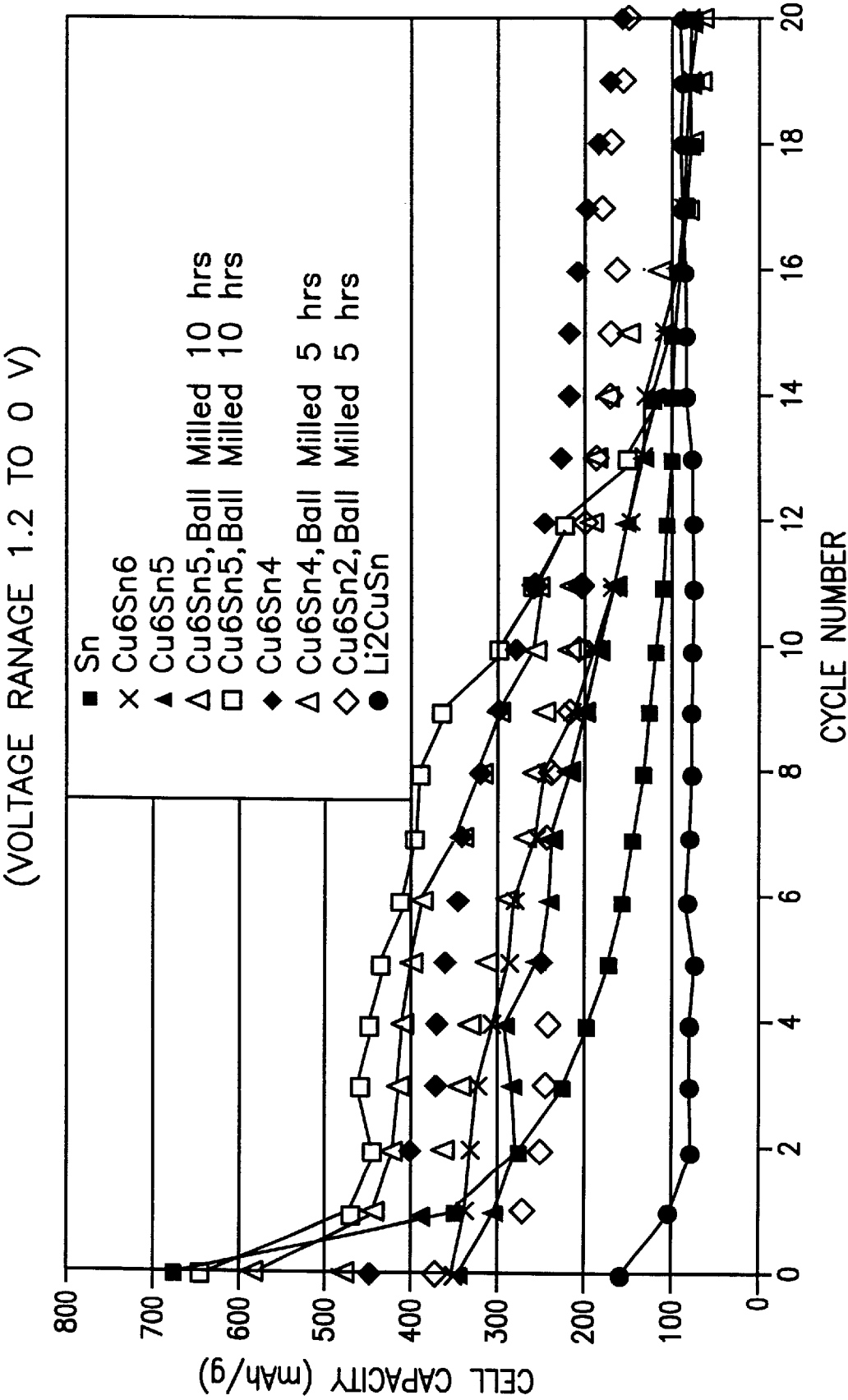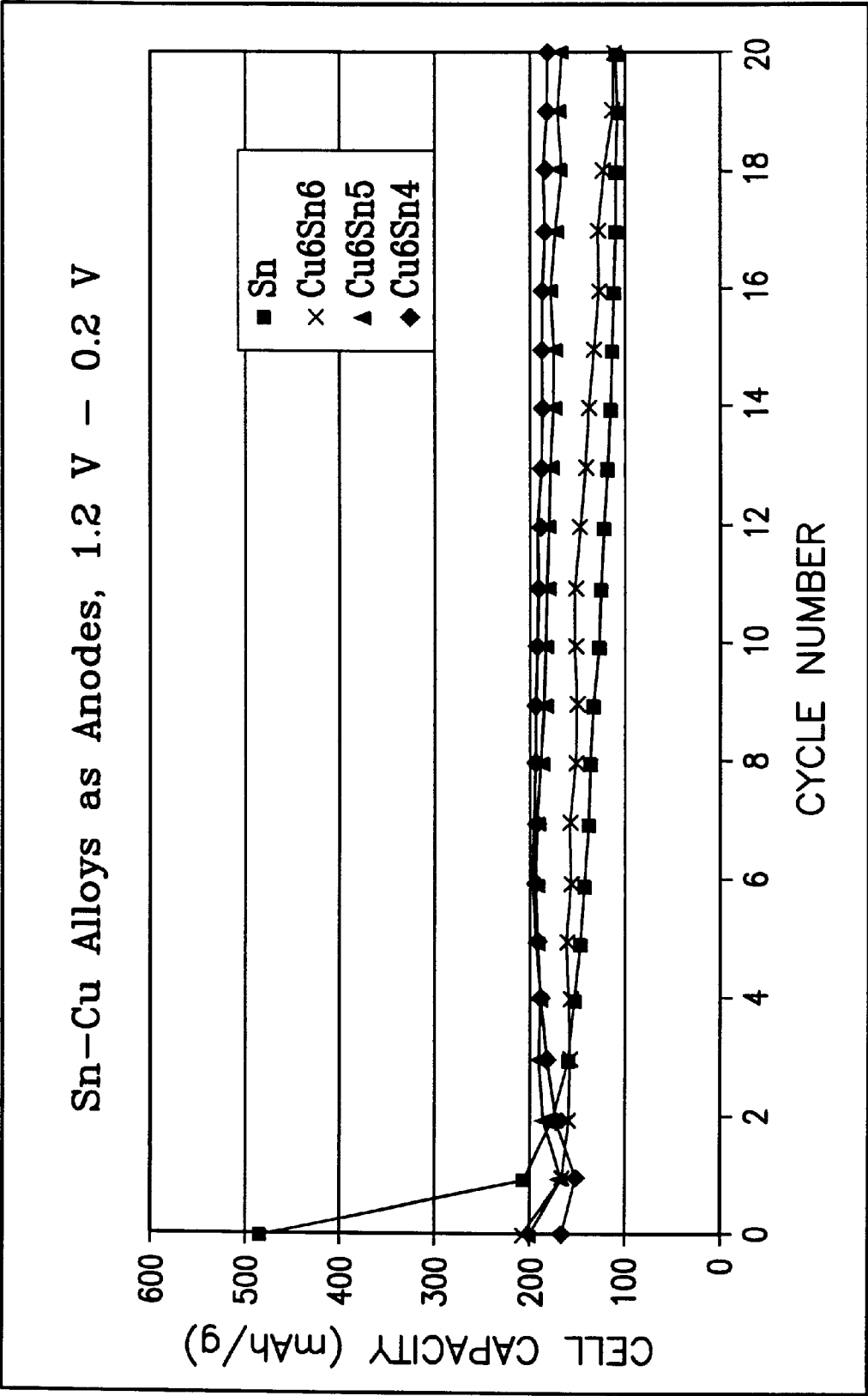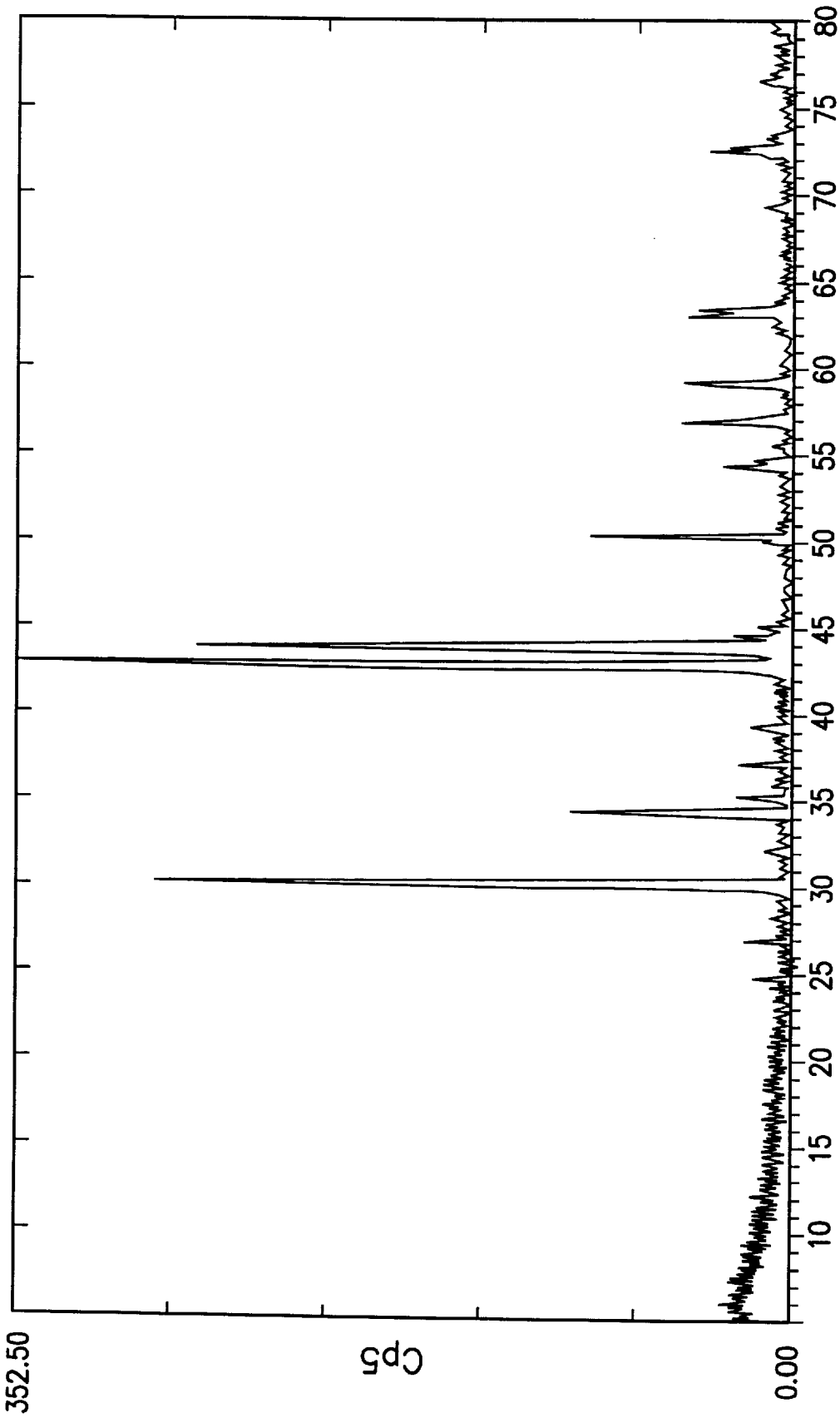
FIG. 21

FIG. 22

FIG. 23

FIG. 24

FIG. 25

FIG. 26

ANODES FOR RECHARGEABLE LITHIUM BATTERIES

RELATED APPLICATIONS

This application is based upon provisional application Ser. No. 60/092,206, filed Jul. 9, 1998, and upon provisional application Ser. No. 60/142,312 filed Dec. 21, 1998, and is a continuation-in-part of PCT application Ser. No. PCT/US99/12868 filed Jun. 8, 1999, and is a continuation-in-part of PCT/US99/18811 filed Aug. 17, 1999 which PCT application was abandoned.

CONTRACTUAL ORIGIN OF THE INVENTION

The United States Government has rights in this invention pursuant to Contract No. W-31-109-ENG-38 between the U.S. Department of Energy (DOE) and The University of Chicago representing Argonne National Laboratory.

BACKGROUND OF THE INVENTION

This invention relates to new anode materials for lithium ion batteries. More specifically this invention relates to new anode materials for lithium-ion batteries consisting of intermetallic materials having active and inactive metals with respect to lithium, such as for ins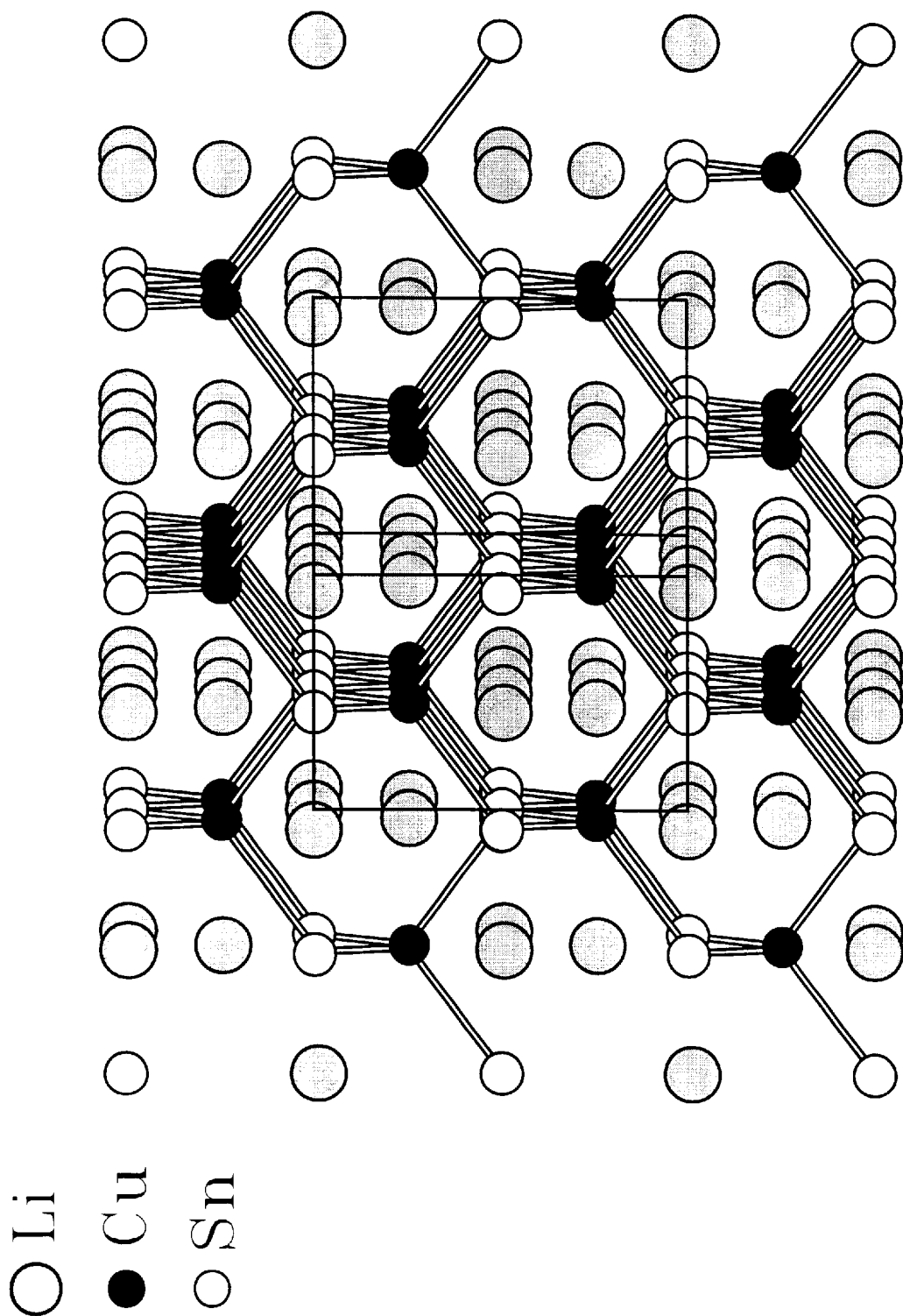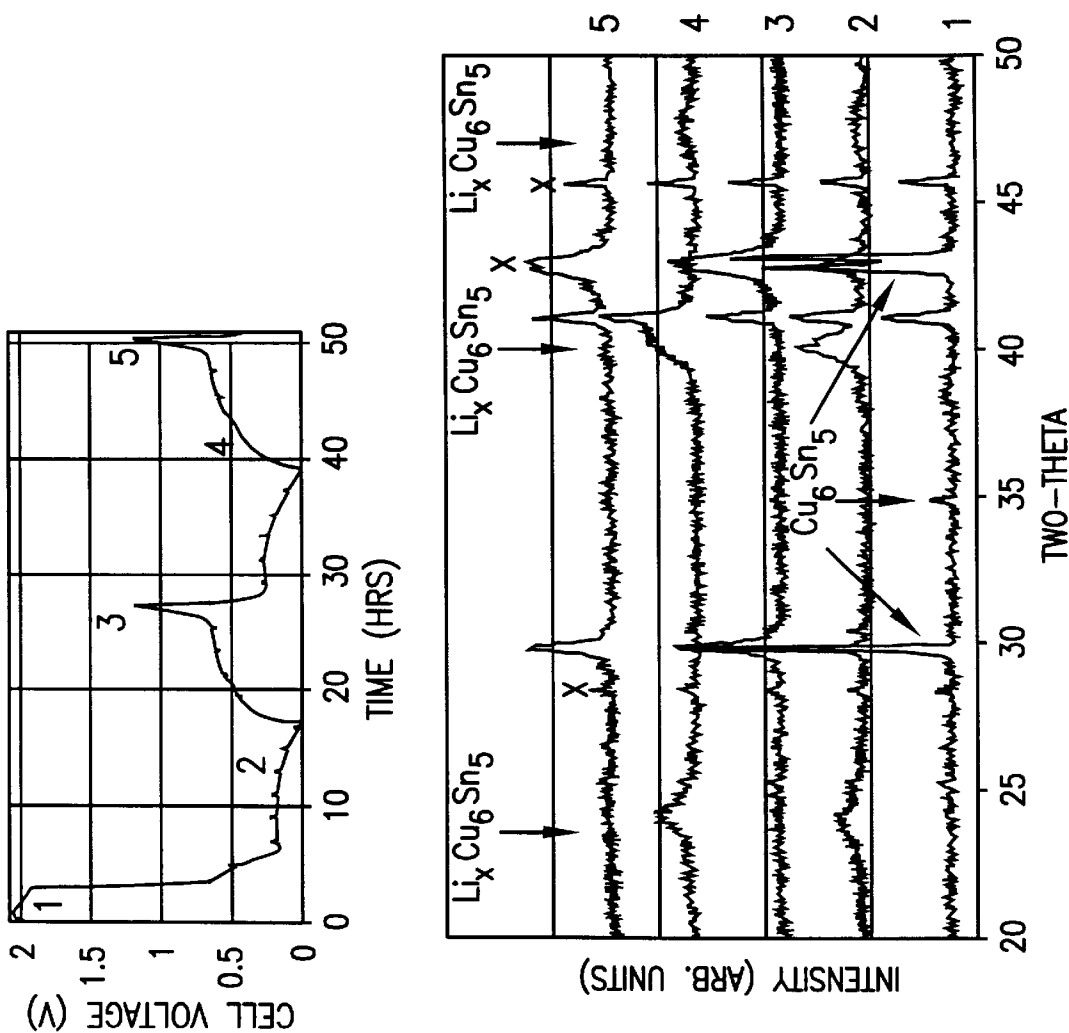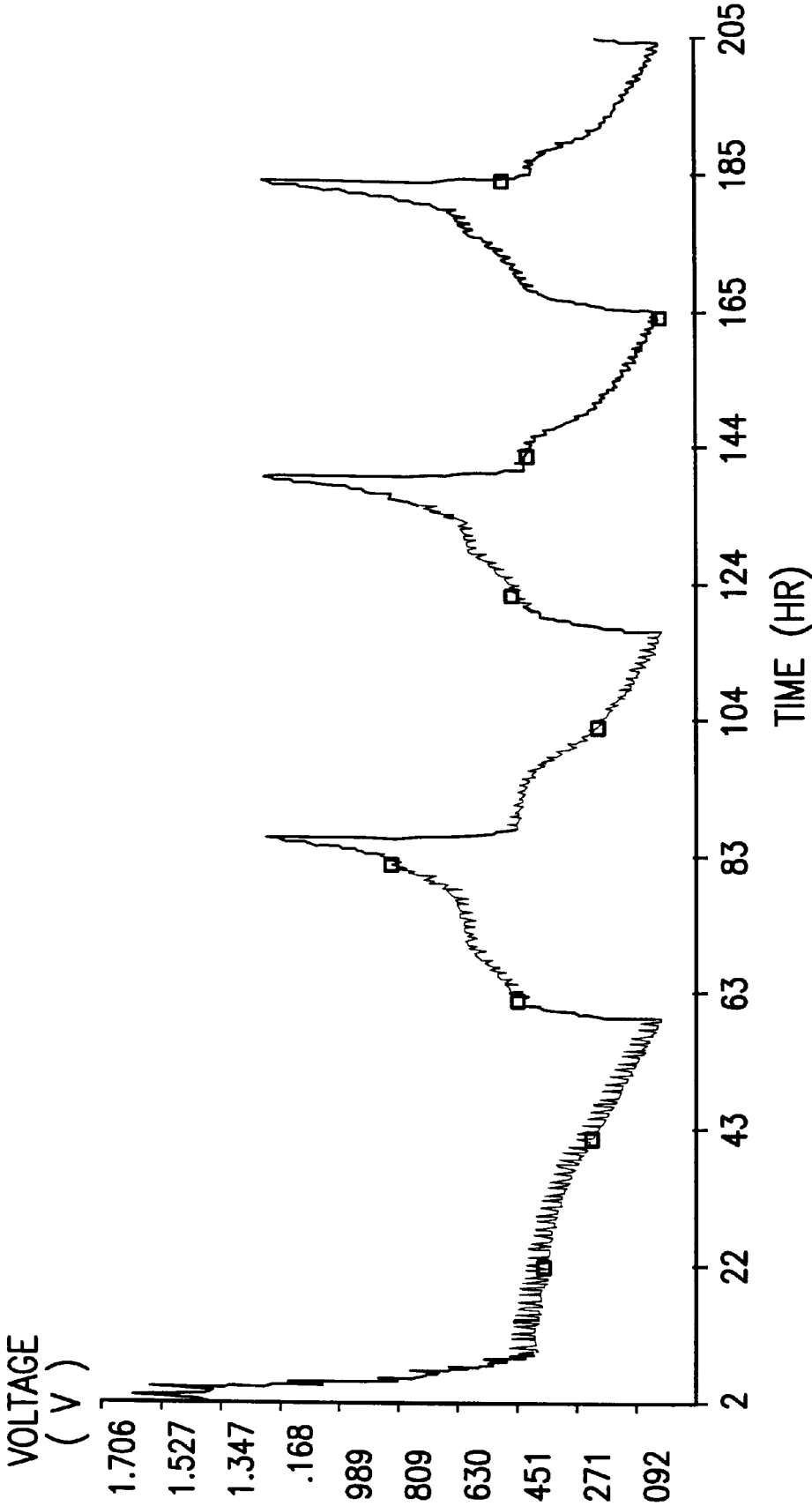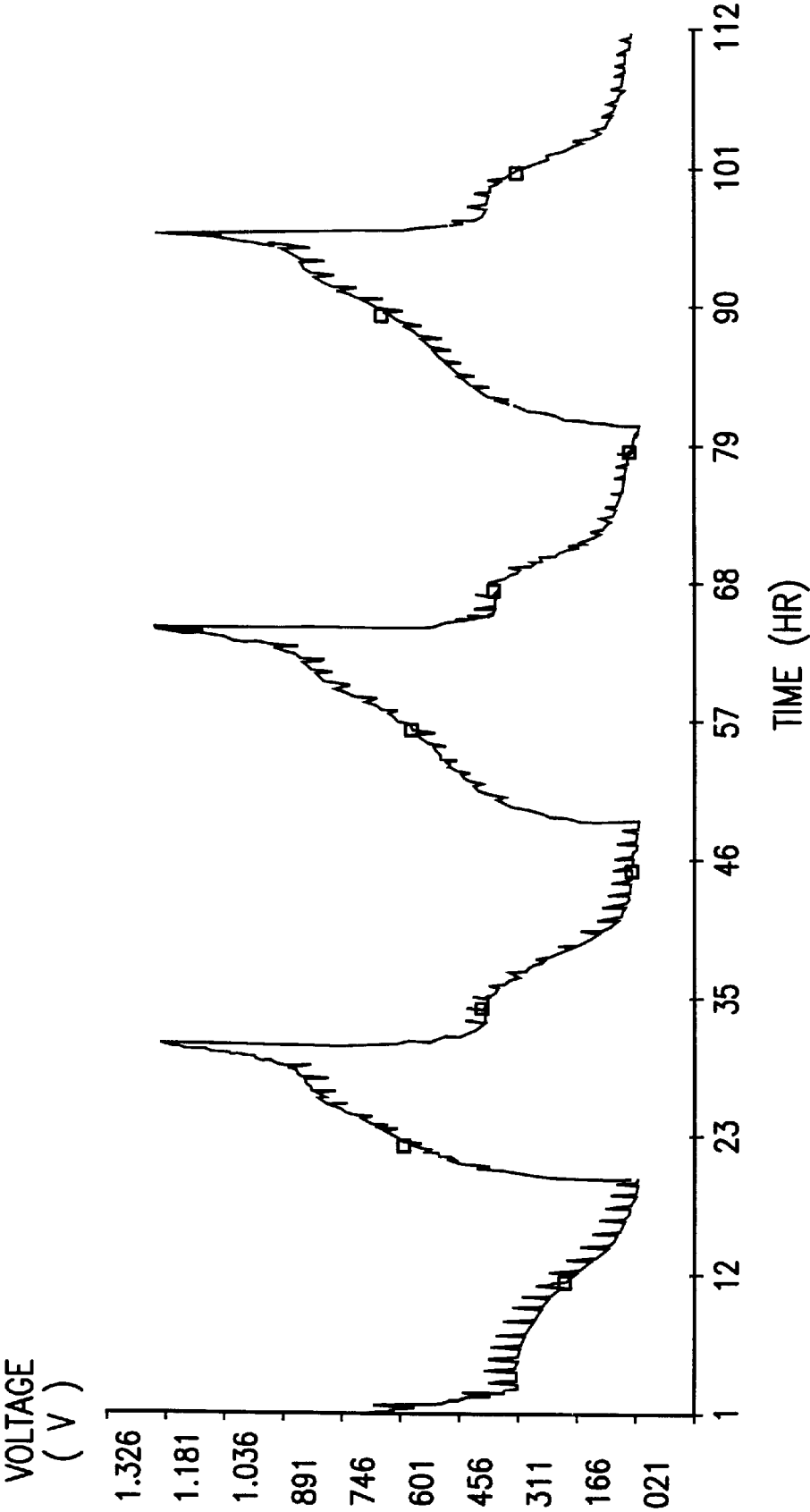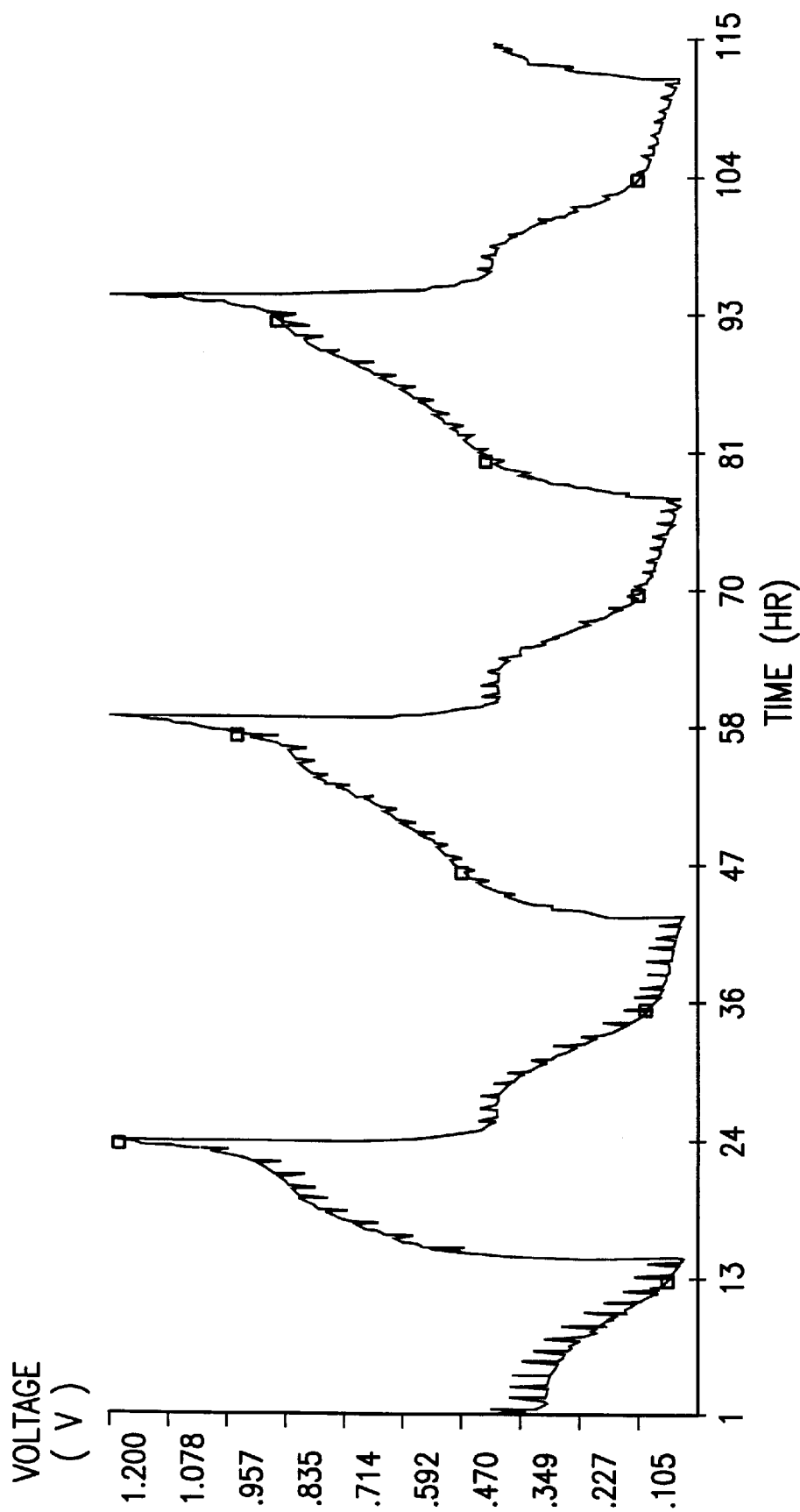tance Sn and Cu metals, respectively. Lithium-ion batteries are under development for the consumer electronics market such as cellular phones, laptop computers, and camcorders. Lithium batteries are also being developed for high energy/power systems such as electric vehicles. A major concern about lithium batteries is safety, primarily when metallic lithium is used as the anode material. This arises because lithium has a very high oxidation potential and thus reactivity in the cell environment. One approach to the safety issue is to use carbon as a host structure for lithium. The carbon can be either graphite or a less crystalline form of pyrolyzed carbon. Lithium-intercalated graphite/carbon electrodes improve the safety of lithium cells, but do not completely overcome the safety problems, because there is still the possibility of depositing metallic lithium at the top of the charge when the voltage of the lithiated carbon/graphite anode approaches that of metallic lithium. Carbon itself when present in a finely divided form with a high surface area, can be highly reactive particularly if oxygen is released within the cell from a highly oxidizing cathode material such as $Li_{1-x}CoO_2$, $Li_{1-x}NiO_2$, and $Li_{1-x}Mn_2O_4$.

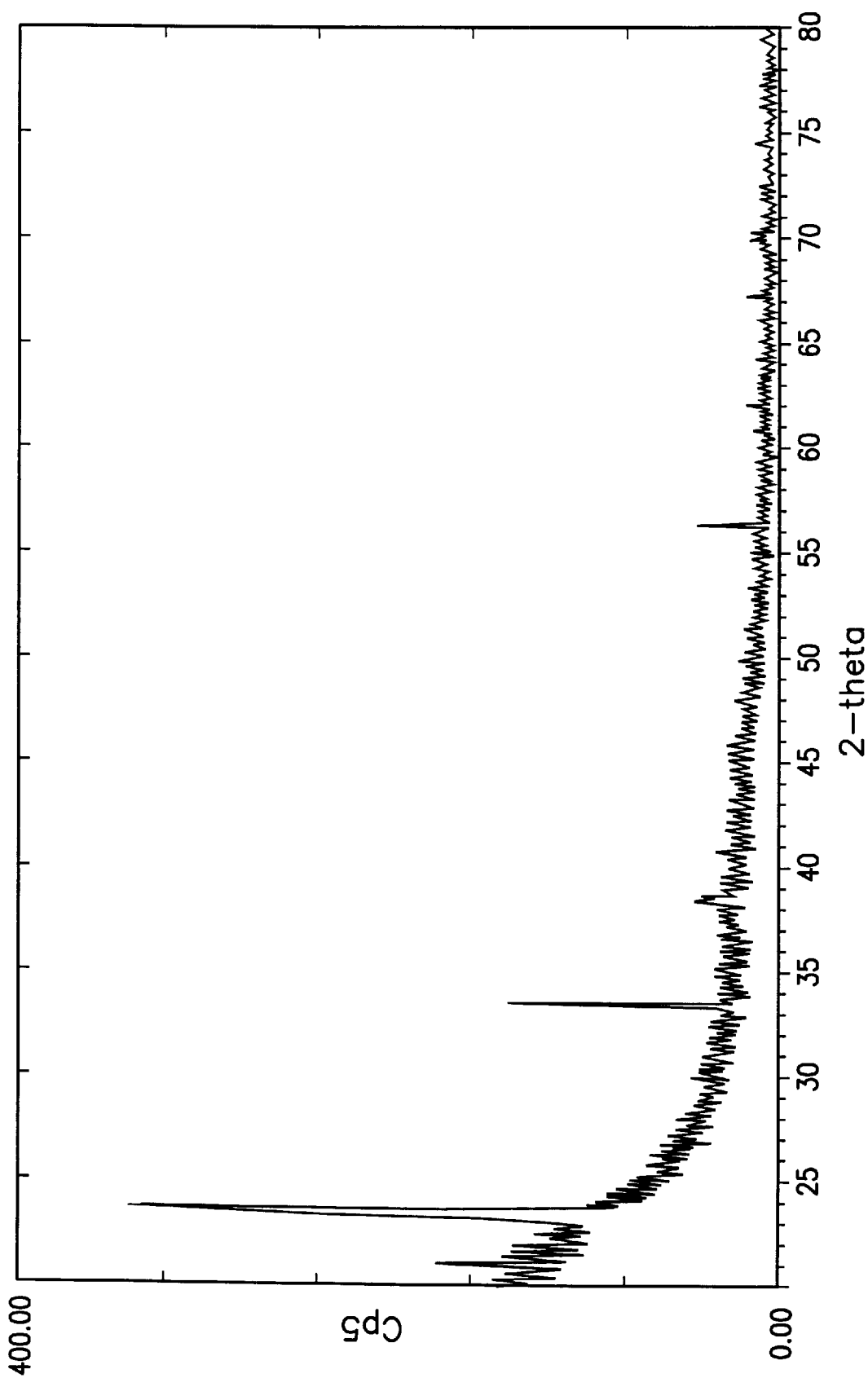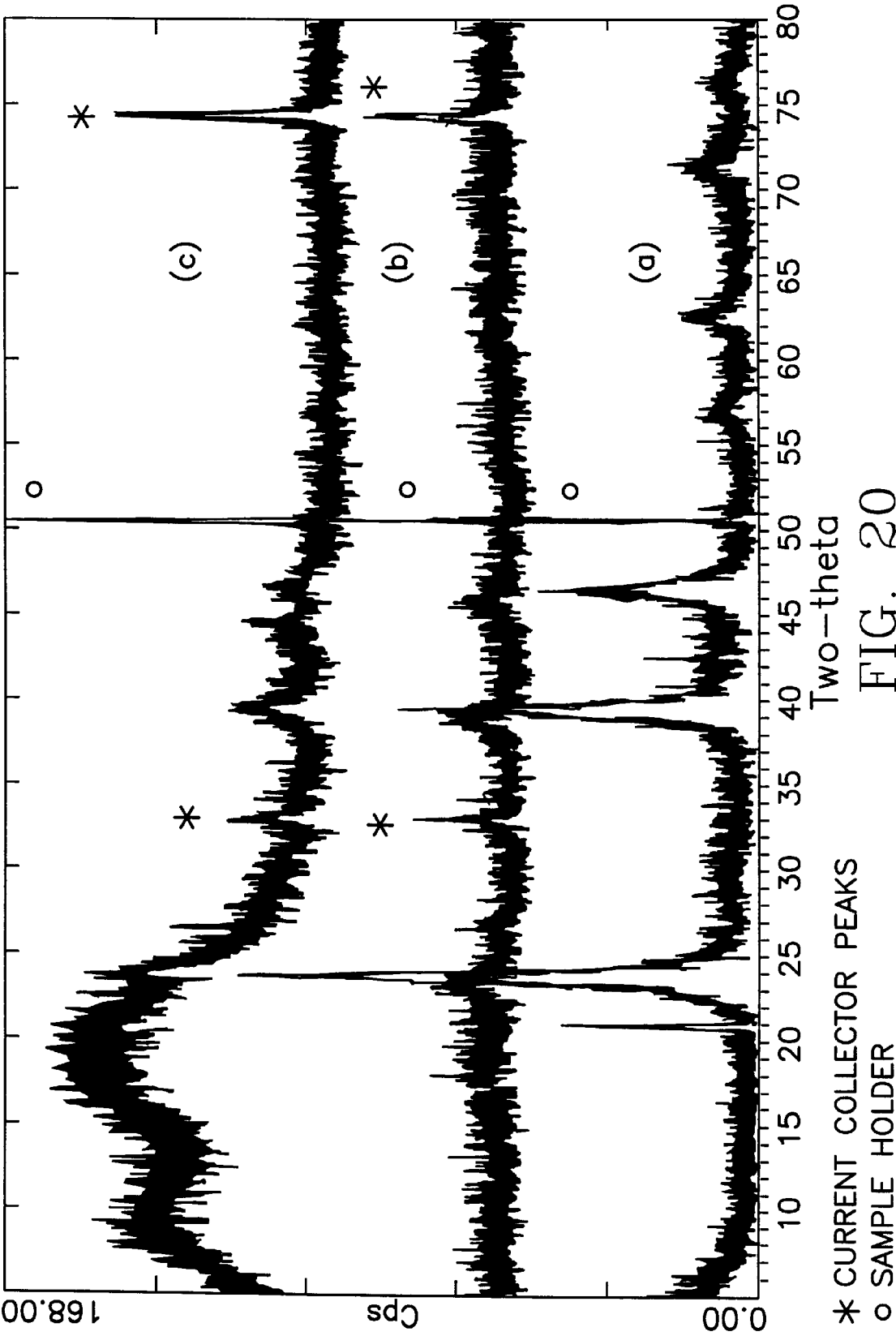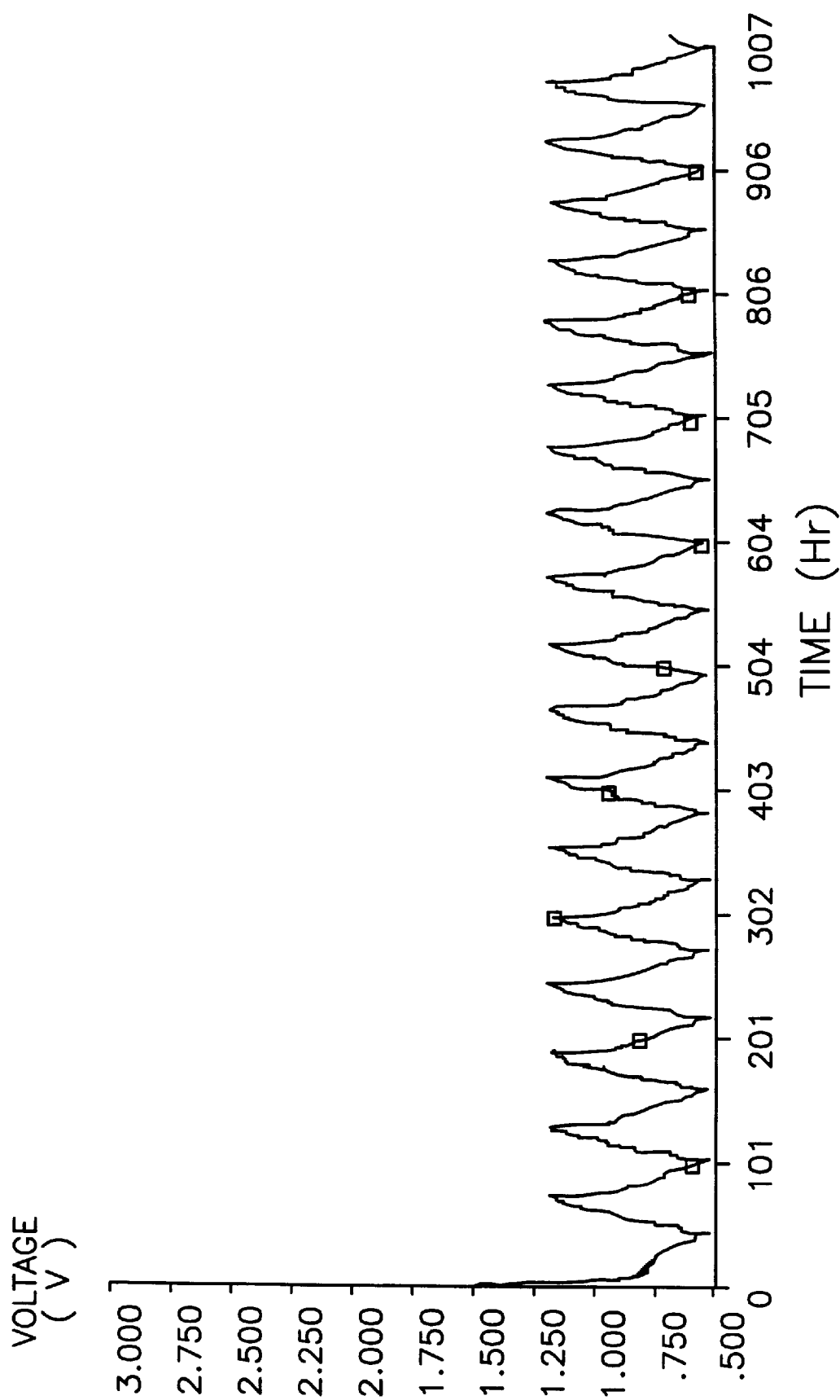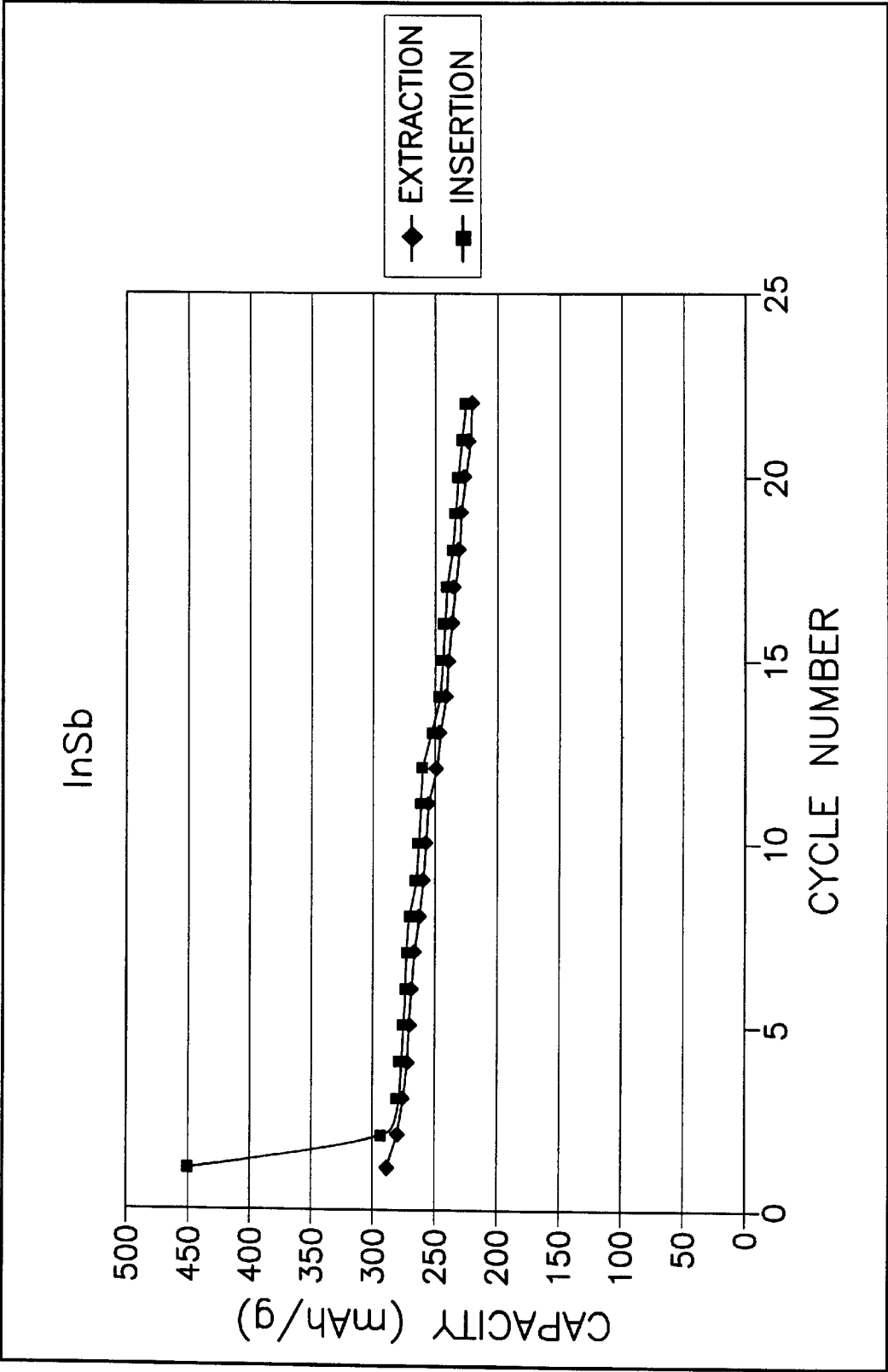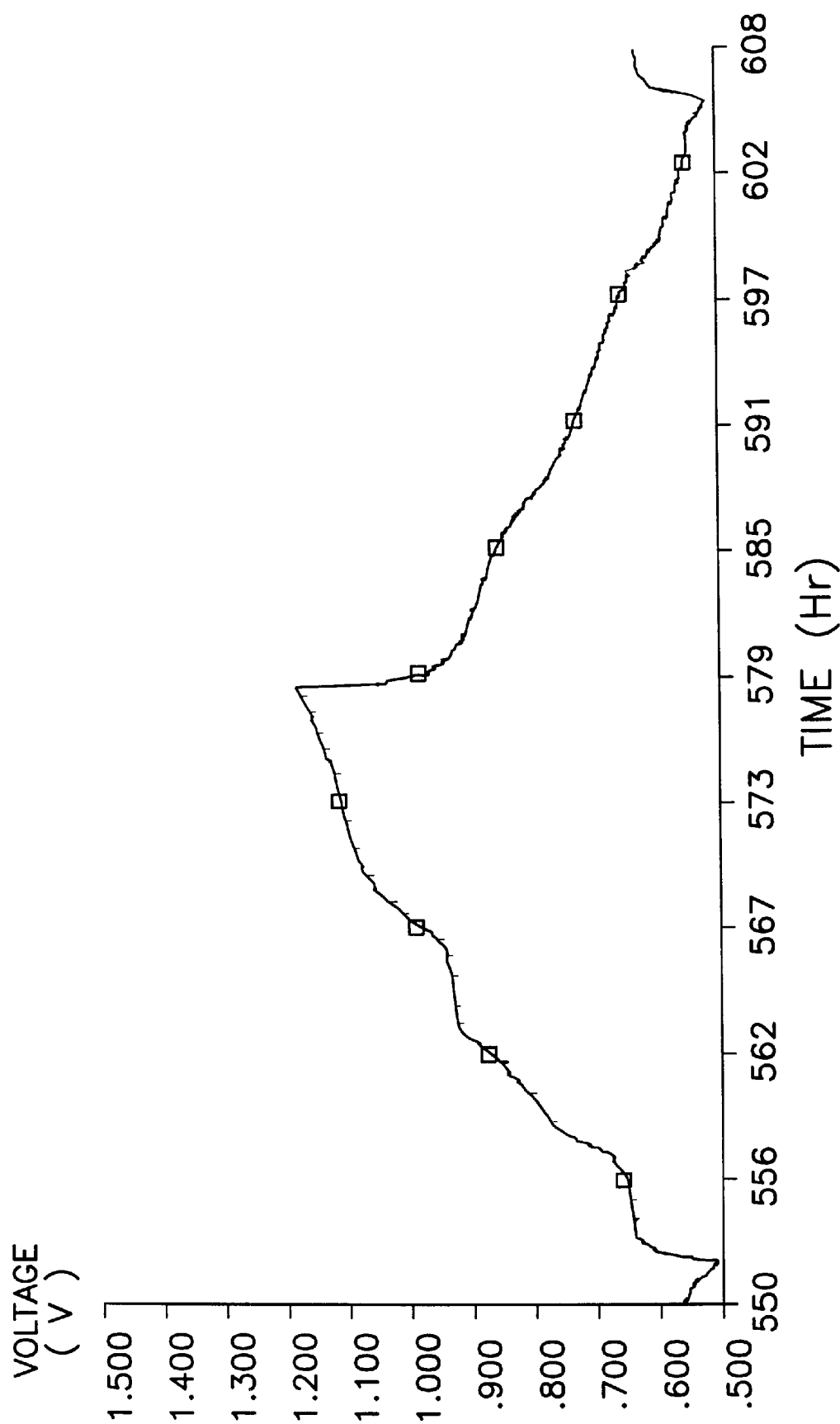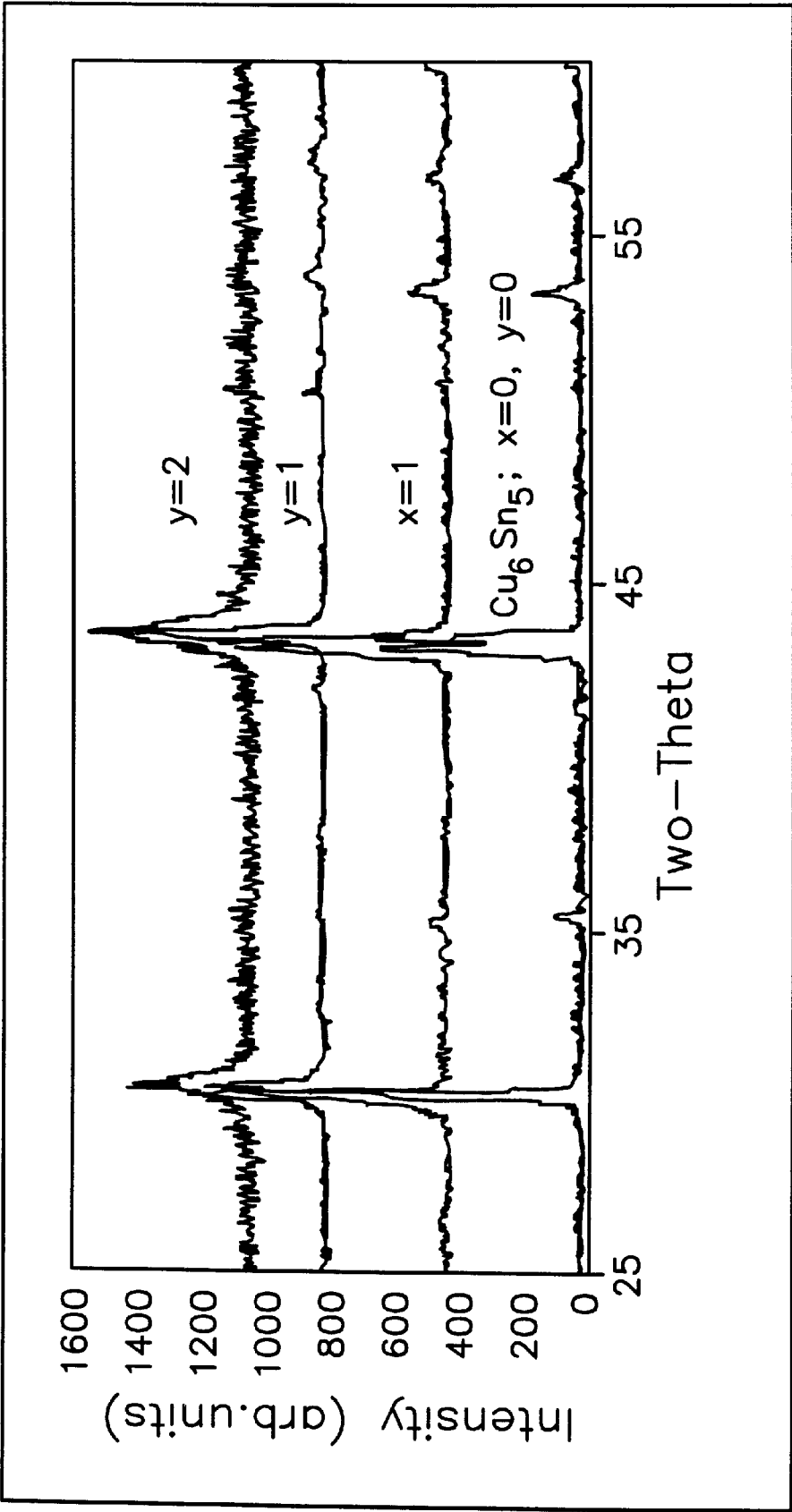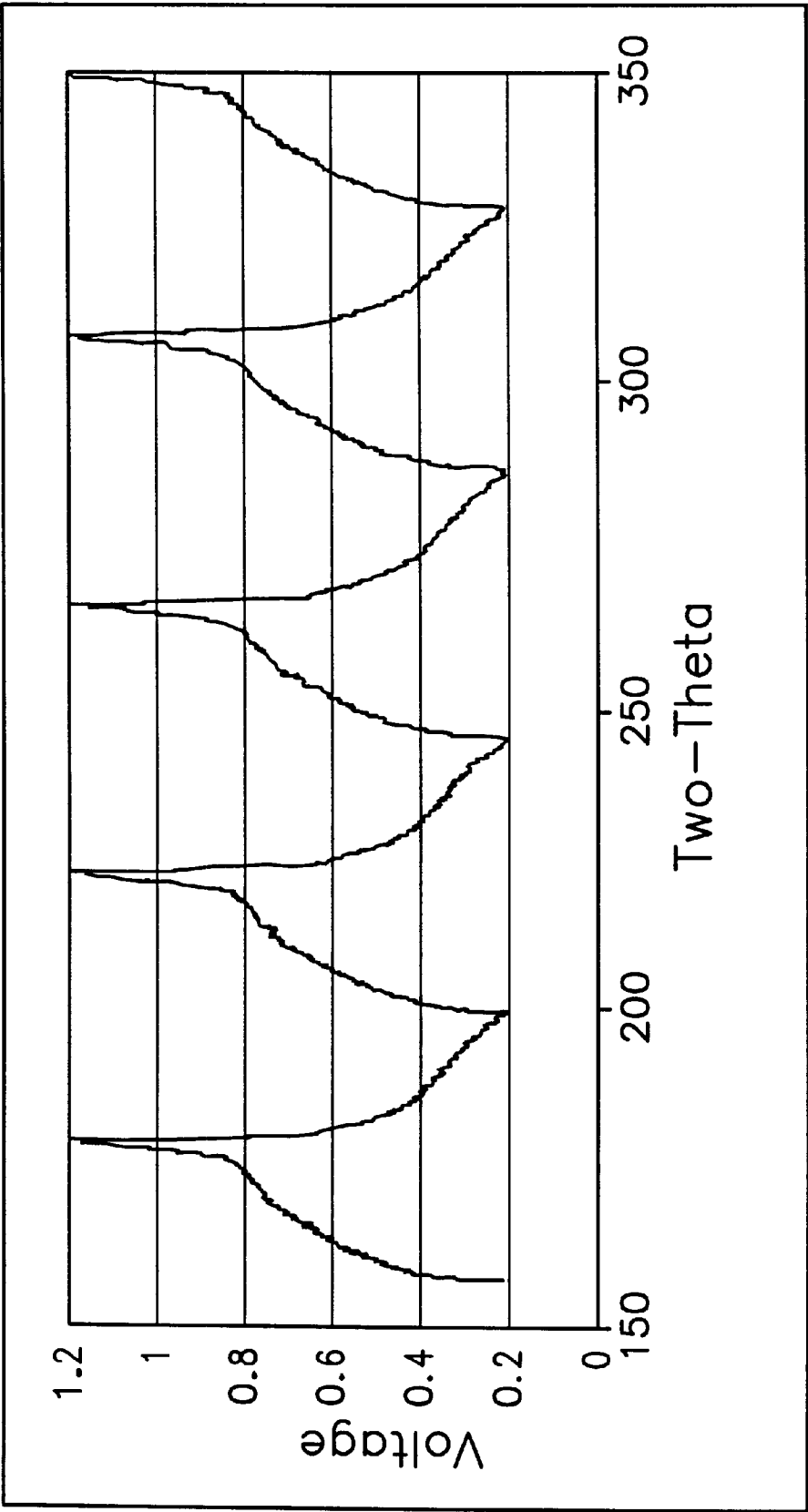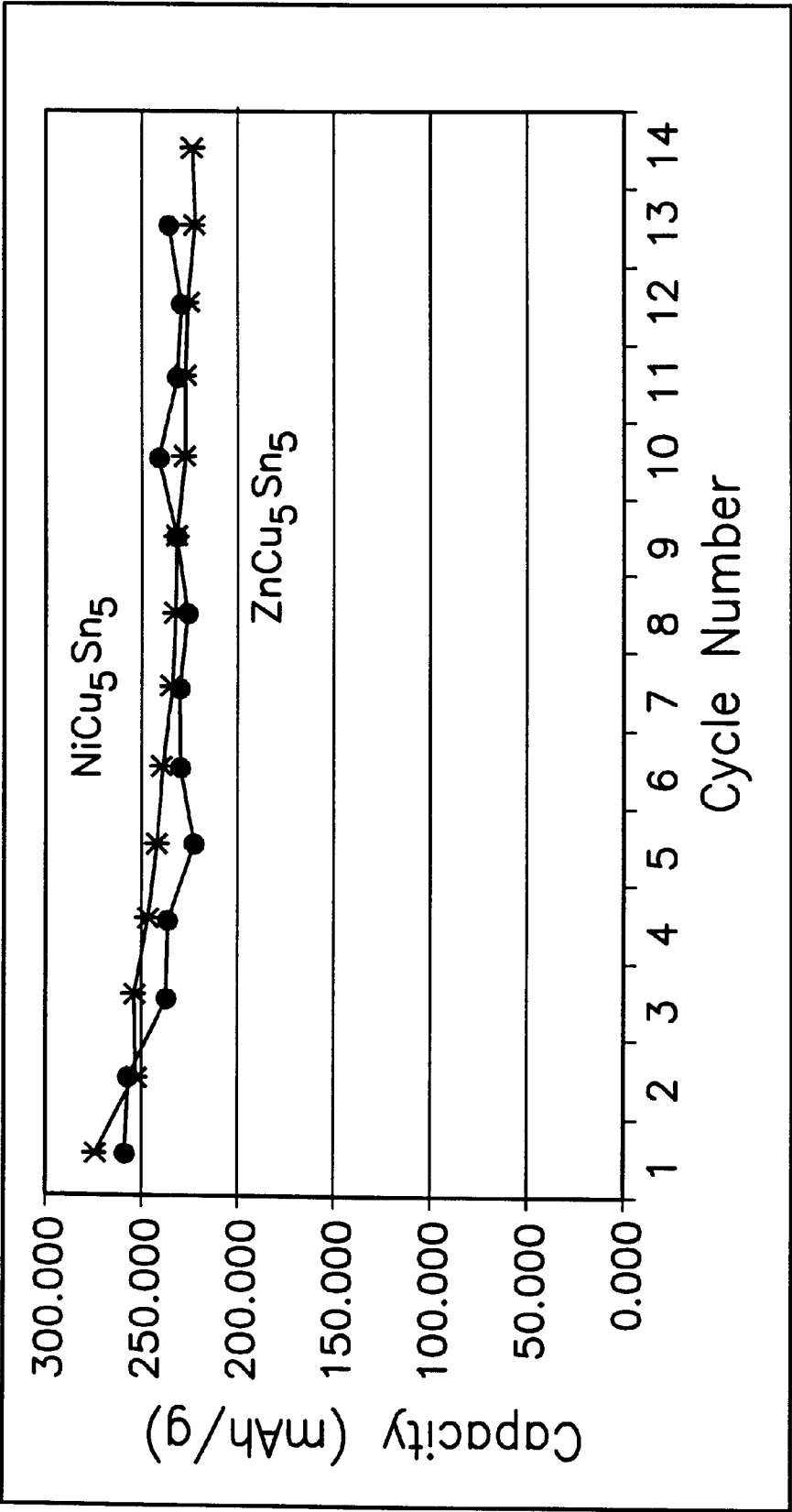There is, therefore, a need to find alternative anode materials to carbon. Many binary lithium alloy systems, such as Li_xAl, Li_xSi and Li_xSn have been extensively studied in the past. These alloys undergo several phase transitions during charge and discharge; the structures undergo severe lattice expansion and contraction that limits the cycle-life of the electrode. An improvement in cycle-life has been made by using an amorphous tin oxide negative (anode) electrode, in which the tin ions are initially reduced to a metallic state (during the charge process of lithium-ion cells), and thereafter alloyed with lithium to form a series of phases within the Li_xSn system ($0 < x \leq 4.4$). Several high-temperature phases are known, in order of increasing lithium content, they are: Li_2Sn_5, $LiSn$, Li_7Sn_3, Li_5Sn_2, $Li_{13}Sn_5$, Li_7Sn_2 and $Li_{22}Sn_5$; they are generated during the electrochemical reaction of lithium with tin at 400° C. At 25° C., the electrochemical profile has indicated that the compositions of the stable phases are Li_2Sn_5, Li_2Sn_3, Li_7Sn_3, Li_5Sn_2, Li_7Sn_2 and $Li_{22}Sn_5$. Tin-oxide electrodes suffer an irreversible capacity loss on the first cycle because a significant amount of the lithium is trapped within the charged electrode as lithium

oxide. Furthermore, lithium oxide is an insulator, which reduces the electronic conductivity of the electrode, a serious disadvantage since for optimum performance the anode needs to be an electrical conductor.

SUMMARY OF THE INVENTION

We have invented a new anode for a lithium battery by replacing the oxygen of a tin oxide electrode with a metal such as copper, which has not only excellent electrical properties, but also has a low oxidation potential, and therefore a low reactivity in a lithium cell environment; copper foil is also used as the current collector at the negative electrode in conventional $Li_xC_6/Li_{1-x}CoO_2$ lithium-ion cells. More generally, the invention relates to the use of intermetallic compounds, based on the structure types of copper-tin and lithium-copper-tin materials, as defined by their relationship to NiAs type, Ni_2In type and lithiated zinc-blende-type materials as anode materials for rechargeable lithium batteries. The invention also includes nonaqueous electrochemical cells incorporating the new anodes and the methods of making the anodes and cells. In the anode, there is one or more of an active metal which can alloy substantially with lithium (such as tin) and, in most instances, there is one or more of an inactive metal which does not substantially alloy with lithium (such as copper). There are other examples in which the anode material components consist of two (or more) active metals that can alloy with lithium, such as tin and germanium.

The invention also includes cells and batteries incorporating the new anode materials with standard state-of-the-art cathodes such as lithium cobalt oxide, lithium nickel oxide or lithium manganese oxides (and various substituted oxides), cathodes now useful in lithium rechargeable batteries.

BRIEF DESCRIPTION OF THE DRAWINGS

The invention consists of certain novel features and a combination of parts hereinafter fully described, illustrated in the accompanying drawings, and particularly pointed out in the appended claims, it being understood that various changes in the details may be made without departing from the spirit, or sacrificing any of the advantages of the present invention.

FIG. 1 depicts a schematic illustration of an electrochemical cell;

FIG. 2 is a representation of the ideal structure of a high-temperature Cu_6Sn_5 intermetallic compound, labeled η-Cu_6Sn_5;

FIG. 3 is a representation of the ideal structure of NiAs;

FIG. 4 is a representation of the ideal structure of Ni_2In;

FIG. 5a is a [001] crystallographic projection of the high-temperature structure of η-Cu_6Sn_5 shown in FIG. 2 showing the displacement of Sn atoms that is required for the transformation to a cubic $Li_xCu_6Sn_5$-type structure ($x_{max} \sim 13$);

FIG. 5b is a [001] crystallographic projection of the ideal structure of the room-temperature Cu_6Sn_5 intermetallic compound, labeled η'-Cu_6Sn_5, showing the displacement of Sn (or Cu) atoms that is required for the transformation to a cubic $Li_xCu_6Sn_5$-type structure;

FIG. 6 is a [001] crystallographic projection of the ideal structure of the Ni_3Sn_2 (and Co_3Sn_2) intermetallic compound;

FIG. 7 shows the X-ray diffraction patterns (CuK radiation) of a) a standard Cu_6Sn_5 sample at room-

temperature, b) $Li_xCu_6Sn_5$ obtained by electrochemical insertion of lithium at room temperature, c) a standard Li_2CuSn sample at room temperature, and d) a chemically delithiated sample of Li_2CuSn at room temperature;

FIG. **8a** is a representation of the ordered room-temperature structure of Li_2CuSn;

FIG. **8b** is a representation of the disordered high-temperature structure of Li_2CuSn;

FIG. **8c** is a representation of the zinc-blende type CuSn framework of the Li_2CuSn structure shown in FIG. **8a**;

FIG. **9** is a [001] crystallographic projection of the ordered structure of Li_2CuSn shown in FIG. **8a**;

FIG. **10** shows the in-situ X-ray diffraction data (CuK radiation) of a $Li/Li_xCu_6Sn_5$ cell;

FIG. **11** is an electrochemical profile of the first four discharge and three charge cycles of a Li/Sn cell between 1.2 volts and 0.0 volts;

FIG. **12** is a graphical representation similar to FIG. **11** for a Li/Cu_6Sn_6 cell;

FIG. **13** is a graphical representation similar to FIG. **11** for a Li/Cu_6Sn_5 cell;

FIG. **14** is a graphical representation similar to FIG. **11** for a Li/Cu_6Sn_4 cell;

FIG. **15** is a graphical representation similar to FIG. **11** for a Li/Li_2CuSn cell;

FIG. **16** is a graphical representation showing the relationship between cell capacity and the first twenty cycles for Li/Sn, $Li/Cu_6Sn_{5+\delta}$ (where $\delta=0,+1,-1,-3$) and Li/Li_2CuSn cells cycled between 1.2 volts and 0.0 volts;

FIG. **17** is a graphical representation similar to FIG. **16** for Li/Sn and $Li/Cu_6Sn_{5+\delta}$ (where $\delta=0,+1,-1$) cells cycled between 1.2 volts and 0.2 volts;

FIG. **18** shows the X-ray diffraction pattern (CuK radiation) of a Ni_3Sn_2 sample at room-temperature;

FIG. **19** shows the X-ray diffraction pattern (CuK radiation) of a Li_2AgSn sample at room-temperature;

FIG. **20** shows the X-ray diffraction patterns (CuKα radiation) of (a) an InSb sample at room temperature, (b) a Li_xInSb electrode lithiated to 0.5 V vs. Li_x and (c) a cycled Li_xInSb electrode after lithium extraction to 1.2 V vs. Li;

FIG. **21** is a graphical representation similar to FIG. **11** for the first 18 cycles of a Li/InSb cell cycled between 1.2 volts and 0.5 volts;

FIG. **22** is a graphical representation similar to FIG. **16** for the first 22 cycles of a Li/InSb cell cycled between 1.2 volts and 0.5 volts;

FIG. **23** is an expanded graphical representation similar to FIG. **21** for the 10th cycle of a Li/InSb cell cycled between 1.2 volts and 0.5 volts;

FIG. **24** shows the X-ray diffraction patterns (CuKα radiation) of a zinc-substituted Cu_6Sn_5 structure, $Cu_{6-x}Zn_xSn_5$, with x=1, and two nickel-substituted Cu_6Sn_5 structures, $Cu_{6-y}Ni_ySn_5$, with y=1 and 2;

FIG. **25** is a graphical representation similar to FIG. **11** for 4 cycles of a $Li/Cu_{6-x}Zn_xSn_5(x=1)$ cell; and

FIG. **26** is a graphical representation similar to FIG. **16** for the first 13 and 14 cycles of a $Li/Cu_{6-x}Zn_xSn_5$ (x=1) cell, and a $Li/Cu_{6-y}Ni_ySn_5$ (y-1), respectively, where the dot (·) is Zn, and the star (*) is Ni.

DETAILED DESCRIPTION OF THE INVENTION

As prebiously stated, the invention relates to a new anode for use in an electrochemical cell **10** having an anode **12**

separated from a cathode **16** by an electrolyte **14**, all contained in an insulating housing **18** with suitable terminals (not shown) being provided in electronic contact with the anode **12** and the cathode **16**, as shown schematically in FIG. **1**. Binders and other materials normally associated with both the electrolyte and the anode and cathode are well known and are not described herein, but are included as is understood by those of ordinary skill in this art.

The anodes of the present invention include intermetallics comprising a substantially active element (or elements) which alloys with lithium with a substantially inactive element (or elements) which does not alloy with lithium, or alternatively, comprising a combination of substantially active alloying elements, the anodes having structure types based on the copper-tin compound Cu_6Sn_5 and lithium-copper-tin derivatives, such as the compound Li_2CuSn. Metals which are considered active, that is metals which can form a binary alloy with lithium useful in this invention are preferably one or more of Sn, Si, Al, Ga, Ge, In, Bi, Pb, Zn, Cd, Hg and Sb. The substantially inactive elements which do not form substantial binary alloys with Li are selected preferably from the first row of transition metals and more preferably one or more of Cu, Ni, Co, Fe, M, Cr, Ti, V and Sc, and in addition, Mg and Ag along with the noble metals, Pd, Rh, and Ir. More specifically, the preferred combinations of inactive and active metals are Cu and Ni, and one or more of Sn, Ge, Sb, Si and Al. It is understood that the active and inactive metals may be present in a wide variety of ratios as will hereinafter be described with the Cu_6Sn_5 and Li_2CuSn intermetallic compounds, by way of example only. It should be understood that various combinations, relative amounts and relative "activities" of both the inactive metals and the active metals may be used in the context of intermetallic compounds without departing from the true spirit and scope of the present invention.

By way of example only, we selected the eta-phase Cu_6Sn_5 and the intermetallic phase Li_2CuSn to demonstrate the principles of this invention; in this invention, we describe in detail the structural properties and electrochemical properties of $Cu_6Sn_{5+\delta}$ ($\delta=-3, -1, 0, +1$) and Li_2CuSn electrode materials in cells with metallic lithium electrodes.

The concept of using an intermetallic compound, MM', where M is an "active" alloying element and M' is an "inactive" element (or elements) can be considered, broadly speaking, analogous on a macroscopic scale to a metal oxide insertion electrode, such as MnO_2 in which Mn is the electrochemically active ion and O is the inactive ion. In an MnO_2 host electrode, lithium ions are inserted into the structure to a composition $LiMnO_2$ with a concomitant reduction of the manganese ions from a tetravalent to a trivalent state. In MnO_2, the ratio of the inactive element to active element is 2:1; for the uptake of one lithium ion per manganese ion, the capacity of the MnO_2 electrode is 308 mAh/g. Manganese oxides, such as the spinel-related phase, λ-MnO_2, that expand and contract isotopically during lithium insertion and extraction with minimal volume expansion of the unit cell provide greatly enhanced cycling stability compared to manganese oxide structures that expand and contract anisotopically with a large volume increase, as in the ramsdellite-Li_xMnO_2 structure.

In an intermetallic system such as Cu_6Sn_5, the tin atoms can be regarded, broadly speaking, as the electrochemically active component (because it forms a binary Li_xSn alloy system with Li) and the copper atoms as the inactive component, (because it does not substantially alloy with Li). Lithium insertion into the Cu_6Sn_5 structure takes place initially in a topotactic reaction to yield a structure, believed

to have the nominal composition $Li_{13}Cu_6Sn_5$, or $Li_{2.17}CuSn_{0.83}$, i.e., with a maximum of 13 Li per Cu_6Sn_5 formula unit, which is approximately the same as that of Li_2CuSn. Thus during the reaction, the Cu_6Sn_5 structure provides a host framework for the uptake of lithium. It is believed that further reaction with lithium necessitates a displacement reaction and a break-up of the $Li_xCu_6Sn_5$ structure; the lithium combines with the active tin to form a series of Li_xSn compounds ($0<x\leqq4.4$) within a residual copper matrix. In this latter-type reaction, the divided copper atoms/particles that are produced on electrochemical cycling would provide an electronically conducting matrix to contain the lithiated tin particles and to accommodate at least some of the damaging expansion/contraction of the Li_xSn particles during discharge and charge (note that in a Li/Cu_6Sn_5 cell, extensive discharge means the formation of a "$Li_xCu_6Sn_5$" composite electrode (with $x>\sim13$) consisting of domains of lithiated tin and copper metal). Optimum cycling conditions would be expected from such a composite Cu/Li_xSn material if it had an ideal microstructure in which the Cu and Li_xSn particles were evenly distributed with sufficient porosity to accommodate the reacted lithium, thus allowing a minimal isotropic expansion of the overall electrode. Although it is believed that the initial topotactic reaction provides a $Li_xCu_6Sn_5$ electrode with superior cycling behavior compared to the subsequent displacement reaction, the invention also includes the composite electrodes that are derived over longer-term cycling by the displacement reaction described above and which can yield higher capacities than can be obtained from the topotactic reaction alone.

The Cu_6Sn_5 structure exists in a high temperature form and a low temperature form. The transition from the one form to the other takes place at 460K as previously reported. The high-temperature structure of Cu_6Sn_5, labeled η-Cu_6Sn_5 and shown in FIG. 2, was first reported in 1928 to have the NiAs-type structure. Simplistically, η-Cu_6Sn_5 has a defect NiAs structure in which the Cu atoms adopt the octahedral sites occupied by Ni in NiAs, and the Sn atoms occupy the trigonal prismatic sites adopted by As; there is one vacant trigonal prismatic Sn site per Cu_6Sn_5 unit. A recent analysis in 1994, of the room-temperature Cu_6Sn_5 structure, labeled η'-Cu_6Sn_5, has shown that this compound has features of both a NiAs-type and a Ni_2In-type structure.

In the well known NiAs structure, which has a hexagonal-close-packed ABACABAC arrangement of atoms (FIG. 3a), the Ni atoms are octahedrally coordinated to six As atoms, whereas the As atoms are coordinated in trigonal prismatic manner to six Ni atoms. The [001] crystallographic projection of the NiAs structure in FIG. 3 shows that the Ni and As atoms are arranged in strings. There are twice as many As strings as Ni strings. The Ni strings are densely packed, whereas the As strings contain half as many As atoms as there are Ni atoms in the Ni strings. In FIG. 3, the NiAs structure is seen to consist of an array of hexagonal columns, each column consisting of alternating Ni strings and As strings, and each column containing an As string at its center.

The [001] crystallographic projection of the Ni_2In structure is shown in FIG. 4. In this structure, there is a similar hexagonal arrangement of atom strings as described for NiAs (FIG. 3). In Ni_2In, however, strings of Ni atoms (octahedrally coordinated to surrounding In atoms) alternate with strings containing both In and Ni atoms to make up the hexagonal columns. In the In—Ni strings, the In atoms have trigonal prismatic coordination to the Ni atoms in neighboring strings; the Ni atoms in the In—Ni strings reside midway between the In atoms in trigonal bipyramidal interstices

(with respect to neighboring In atoms) to provide a very dense structure (ρ=9.902 g/ml). Each hexagonal column contains, at its center, a similar string of In and Ni atoms.

The close relationship between the high- and low-temperature forms of the Cu_6Sn_5 structure and the NiAs and Ni_2In structures can be seen in FIGS. 3, 4, 5a and 5b. In the [001] crystallographic projection of the high-temperature modification, η-Cu_6Sn_5, shown in FIG. 5a, the Cu atoms and the Sn atoms are arranged in discrete strings, as in the NiAs structure (FIG. 3). In the [001] crystallographic projection of the room-temperature modification, η'-Cu_6Sn_5, shown in FIG. 5b, the Cu atoms are arranged in discrete rows as they are in η-Cu_6Sn_5 (FIG. 5a), but in this structure the Sn strings also contain some Cu atoms; these Cu atoms are located between the Sn atoms in trigonal bipyramidal sites, one-fifth of which are occupied in the structure. In η'-Cu_6Sn_5, there exist hexagonal columns that consist of Cu strings that alternate with Sn—Cu strings; the center of the hexagonal columns contain identical Sn—Cu strings. Thus, η'-Cu_6Sn_5 may be regarded as having a defect Ni_2In-type structure in which 80% of the trigonal bipyramidal sites are vacant. Intermetallic compounds that are assigned either to the NiAs- or the Ni_2In-type structure commonly have a composition between that of NiAs and Ni_2In. A superstructure is formed if the structure is ordered. Examples of such superstructures are found in room-temperature modifications of η'-Cu_6Sn_5, Ni_3Sn_2, and Co_3Sn_2 intermetallic compounds. The [001] crystallographic projection of the Ni_3Sn_2 structure (which is isostructural with Co_3Sn_2) is shown in FIG. 6; it demonstrates that Ni_3Sn_2 (and Co_3Sn_2) is of the same structure type as η'-Cu_6Sn_5 (FIG. 5b). In practice, however, it is believed that these structures are not ideally ordered and that some disorder can exist, for example between the copper and tin atom sites in the Cu_6Sn_5 structures shown in FIGS. 5a and 5b.

An important aspect of this invention is the discovery by combined electrochemical and in-situ X-ray diffraction studies of Cu_6Sn_5 electrodes in lithium cells, that lithium can be inserted topotactically into the Cu_6Sn_5 structure and that this process is reversible. It is believed, however, that the degree to which the lithium insertion reaction takes place is highly dependent on structural features of the intermetallic electrode, such as anti-site disorder and the reaction conditions under which the intermetallic electrodes are made. The X-ray diffraction data of various lithiated and delithiated samples (FIGS. 7a–d) showed that the lithiated phase $Li_xCu_6Sn_5$ (FIG. 7b) has an X-ray pattern similar to that of Li_2CuSn (FIG. 7c). The structure of Li_2CuSn has cubic symmetry. The room-temperature form of Li_2CuSn (space group symmetry F-43 m), shown in FIG. 8a, is ordered. The Sn atoms and one-half of the Li atoms form two interlinked face-centered-cubic arrays. The Cu atoms and remaining Li atoms occupy interstitial sites located at the center of cubes defined by 4 Sn and 4 Li atoms of the face-centered-cubic arrays. The high-temperature phase of Li_2CuSn has higher symmetry, Fm-3 m. In this case, the Li and Cu atoms within the cubes are randomly disordered, as shown in FIG. 8b to provide a Heusler-type phase, such as Ni_2MnGa, in which the Ni atoms occupy the same sites as the disordered Li and Cu atoms in FIG. 8b, and the Mn and Ga atoms occupy the sites of the Sn and remaining Li atoms, respectively.

Of particular note is that the CuSn framework of the ordered Li_2CuSn structure (FIG. 8a) has a zinc-blende-type lattice, as shown in FIG. 8c. Therefore, Li_2CuSn may be regarded as having a lithiated zinc-blende-type structure in which the Li atoms occupy the interstitial sites of the CuSn host framework. The invention thus includes zinc-blende-

type framework structures as insertion electrodes for lithium batteries. Other examples of such a zinc-blendetype framework structure is provided by the AgSn component in Li_2AgSn and by the MgSi component in Li_2MgSi. Additional examples of zinc-blende-type structures are AlSb, GaSb, and InSb. Of particular significance is that by using the zinc-blende framework for an insertion electrode, it is possible to tailor the operating voltage of a lithium cell by changing the metal atoms in the framework.

The ordered Li_2CuSn structure, as depicted in a second representation of the structure in FIG. 9, bears a close relationship to the η'-Cu_6Sn_5 structure (FIG. 5a); this relationship, which is seen in the arrangement of the hexagonal columns, makes it easy to understand the topotactic reaction when lithium is inserted electrochemically into η-Cu_6Sn_5. It is apparent from the X-ray diffraction data in FIG. 10 obtained in-situ in an electrochemical cell that the lithiation process involves a two-phase reaction. The phase transformation from η-Cu_6Sn_5 to the Li_2CuSn-type structure can be understood if lithium insertion into the hexagonal columns of η-Cu_6Sn_5 displaces the Sn atoms from the center of the columns into the trigonal bipyramidal interstitial sites in neighboring Sn strings, as shown by the arrows in FIG. 5a. [Note that fall lithiation of η-Cu_6Sn_5 with an ideal defect NiAs-type structure would result in the composition $Li_{13}Cu_6Sn_5$ (alternatively, $Li_{2.17}CuSn_{0.83}$ or $Li_2Cu\{Sn_{0.83}Li_{0.17}\}$), in which 17% of the Sn sites are occupied by Li.] Such a reaction makes the hexagonal channels (5.6–6.2 Å in diameter) accessible for lithium occupation and creates two interstitial sites per hexagon for the incoming Li atoms (FIG. 9). However, to accommodate the inserted Li atoms, the layers of Cu and Sn atoms shear from their hexagonal-close-packed sequence ABACABAC in the η-Cu_6Sn_5 structure to the cubic-close-packed sequence ABCABC of like atoms in the Li_2CuSn-type structure.

During the transformation from η-Cu_6Sn_5 to $Li_{13}Cu_6Sn_5$, all the Cu atoms and one-half of the Sn atoms remain in their original strings. Even though 50% of the Sn atoms are displaced during lithium insertion from one string to another during lithium insertion, the phase transition is topotactic, i.e., a transition in which a definite orientation relationship exists between the two phases and in which some structural reorganization is necessary. In this transformation, one-half of the tin atoms are displaced by approximately 2.7 Å from their trigonal prismatic sites in a two-phase reaction to form columns of tin with the other one-half of the tin atoms. Thus, during this reaction, the "inactive" copper subarray and one-half of the tin subarray of the structure remain spatially intact. In the lithiated product, each Sn atom and each Cu atom is coordinated tetrahedrally to neighboring Cu and Sn atoms, respectively, in a zinc-blende-type structure. This topotactic reaction is reversible. Lithium insertion into the room-temperature structure, η'-Cu_6Sn_5 (FIG. 5b), in which Cu atoms partially occupy 20% of the interstitial trigonal bipyramidal sites can occur by a similar reaction mechanism described for η-Cu_6Sn_5 above. However, in this case, in order to form a Li_2CuSn-type structure, the ideal phase transformation would necessitate the diffusion of Sn atoms in the Sn—Cu strings to interstitial sites in neighboring strings, as shown by the arrows in FIG. 5b. The transformation also necessitates that the Cu atoms diffuse from the Sn—Cu strings to partially occupy the Li sites of an ordered Li_2CuSn-type structure. It is expected, therefore, that the fully-lithiated η'-Cu_6Sn_5 structure would have the composition $Li_9Cu_6Sn_5$, and that the atom arrangement, in Li_2CuSn notation, would be $(Li_{1.8}Cu_{0.2})CuSn$. Because

there are less interstitial sites available in η'-Cu_6Sn_5 compared with η-Cu_6Sn_5, the theoretical gravimetric capacity of η'-Cu_6Sn_5 (248 mAh/g) is significantly less than that of η-Cu_6Sn_5 (358 mAh/g) (Table 1).

Without being bound by theory and by the terminology used to describe the processes by which lithium is inserted into the intermetallic host electrode structures of the invention, the applicants believe that because of the structural relationship between η'-Cu_6Sn_5 (FIG. 5b) and Ni_2In (FIG. 4), lithium insertion into η'-Cu_6Sn_5 may initially occur by the occupation of the interstitial trigonal bi-pyramidal sites by lithium before the transformation to the zinc-blende-type structure. Thus, for η'-Cu_6Sn_5— related materials, including both η-Cu_6Sn_5 and η'-Cu_6Sn_5, the initial lithiated $Li_xCu_6Sn_5$ products can be lithiated to a NiAs-type structure before converting to a lithiated zinc-blende-type structure. The invention is thus extended to incorporate such lithiated NiAs-type structures.

Thus, the discovery of the lithium insertion reaction into Cu_6Sn_5 has immediate important implications for the development of a new family of intermetallic electrodes with the Cu_6Sn_5 and Li_2CuSn structure types. The invention therefore extends to include the family of compounds having structures related to the NiAs, Ni_2In, Cu_6Sn_5 and Li_2CuSn structure types shown in FIGS. 3, 4, 5a, 5b, 8a, 8b and 8c.

For example, the Ni_3Sn_2 (and Co_3Sn_2) structure shown in FIG. 6 is remarkably similar to that of η'-Cu_6Sn_5 (FIG. 5b), having strings of Ni, and strings of Sn—Ni arranged in identical fashion to the strings of Cu and Sn—Cu in η'-Cu_6Sn_5. The difference between Ni_3Sn_2 (Co_3Sn_2) and η'-Cu_6Sn_5 structures is only in the number of interstitial trigonal bipyramidal sites occupied by the Ni (Co) and Cu atoms, respectively, in the Sn strings. For example, in Ni_3Sn_2, 50% of the interstitial trigonal bipyramidal sites are occupied by Ni, in contrast to the 20% occupation by Cu in η'-Cu_6Sn_5. Therefore, using the analogy to η'-Cu_6Sn_5, Ni_3Sn_2 may, in principle, accommodate lithium to the composition $Li_3Ni_3Sn_2$, or in Li_2CuSn notation, to the composition $(Li_{1.5}Ni_{0.5})NiSn$; it offers a lower gravimetric capacity (195 mAh/g) and volumetric capacity (1755 mAh/mi) compared to η'-Cu_6Sn_5 and η'-Cu_6Sn_5 (Table 1). Because of the high number of Ni atoms that must be accommodated in the Li sites of $Li_3Ni_3Sn_2$, it is anticipated that the phase transition should be more difficult to accomplish in $Li_xNi_3Sn_2$ electrodes compared to Cu_6Sn_5 electrodes. This hypothesis is supported by electrochemical data from nickel-tin electrodes that are inferior to the data derived from the analogous coppertin materials. With this structural argument, electrode materials of this invention that are close to the ideal NiAs composition and structure are expected to perform better than those electrodes close to the Ni_2In composition and structure.

In a further embodiment of the invention, Table 2 illustrates the wide variety of compounds that can exist with the Li_2CuSn structure. The hexagonally shaped channels in Li_2CuSn-type structures accommodate the inserted lithium. A particular embodiment of the invention therefore includes those isostructural materials in which non-lithium metals, M, occupy the Cu and Sn atom sites of Li_2CuSn shown in FIG. 8a. One such example is Li_2AgSn, the X-ray diffraction pattern of which is shown in FIG. 19. Another particularly attractive example is Li_2MgSi because Mg and Si are relatively light and inexpensive materials. The invention also includes those structures in which at least some M sites are occupied by Li. This is believed to occur in $Li_xCu_6Sn_5$ electrodes. For example, Cu_6Sn_5 can be represented $CuSn_{0.83}\square_{0.17}$ where $\square$ refers to a vacancy. On lithiation,

therefore, the ideal Li_2CuSn-type structure is reached at the composition $Li_2Cu(Sn_{0.83}Li_{0.17})$, or alternatively $Li_{2.17}CuSn_{0.83}$, or alternatively $Li_{13}Cu_6Sn_5$. In this instance, 17% of the Sn sites are occupied by Li. The reaction of Cu_6Sn_5 with lithium to form $Li_{13}Cu_6Sn_5$ provides an electrode with a theoretical gravimetric capacity and a theoretical volumetric capacities of 358 mAh/g and 2506 mAh/ml, respectively, compared to the theoretical capacities of graphite, viz., 372 mAh/g and 818 mAh/ml (Table 1). A particular advantage of Cu_6Sn_5-type electrodes, therefore, is that they offer a significantly enhanced volumetric capacity to carbon.

It has been demonstrated that it is possible to extract the lithium from the Li_2CuSn structure, both chemically and electrochemically. Complete extraction of lithium would result in a copper-tin electrode with approximately the same CuSn ratio as in η-Cu_6Sn_5. Chemical extraction of lithium with $NOBF_4$ from Li_2CuSn results in a Cu_6Sn_5-type structure, as shown by the strong similarity between the room-temperature X-ray diffraction data of a chemically treated Li_2CuSn sample (FIG. 7d) and a standard Cu_6Sn_5 sample (FIG. 7a). These X-ray diffraction data clearly confirm the reversibility of the reaction

$$xLi+Cu_6Sn_5 \leftrightharpoons Li_xCu_6Sn_5$$
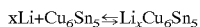
In the high-temperature structure of Li_2CuSn shown in FIG. 8b, the Cu atoms and one half of the Li atoms are disordered over the sites they normally occupy in the ideal, ordered structure at room-temperature (FIG. 8a). In practice, it is believed that at room temperature some disorder exists between these sites. This invention thus extends to include these disordered structures.

In MnO_2, the ratio of inactive element to active element is 2:1 which is approximately twice the ratio in Cu_6Sn_5 (1.2:1). Therefore, it is believed that increasing the inactive copper content as a separate Cu phase in the intermetallic electrode would provide greater cycling stability; conversely, increasing the active tin content as a separate Sn phase probably would reduce the cycling stability of the intermetallic electrode.

$Li/Cu_6Sn_{5+\delta}$ cells were evaluated with electrodes having δ values of −1 (Cu_6Sn_4, copper-rich), 0 (Cu_6Sn_5) and +1 (Cu_6Sn_6, tin-rich). The electrochemical behavior of a standard Li/Sn cell was determined, for comparison. The electrochemical profiles of the first two discharge—and subsequent charge cycles of a Li/Sn cell and $LiCu_6Sn_{5+\delta}$ cells ($\delta=0,\pm1$) charged and discharged between 1.2 and 0.0 V are shown in FIGS. 11–14. All cells show an initial steep drop in voltage followed by a voltage plateau during discharge at approximately 400 mV; the latter process appears to correspond initially to the insertion of lithium into the Cu_6Sn_5 component and on subsequent cycling to the formation of at least some Li_7Sn_3 within a copper matrix. It is believed that reaction beyond the Li_7Sn_3 composition, i.e., when the cell voltage decreases to 0 V, occurs with the successive formation of phases with increasing lithium content, Li_5Sn_2, Li_7Sn_2 and $Li_{22}Sn_5$, as reported for Li/Sn cells at 25° C., but within copper matrix. It can be seen from the current interrupts that occur every hour during discharge and charge that the impedance of each cell improves dramatically after the first discharge. This improvement in performance can be attributed to better contact between electrolyte and active material and improved particle to particle contact that occurs during the early "conditioning" of the cells.

Electrochemical extraction from the intermetallic phase Li_2CuSn occurs with a steadily increasing voltage to the cut-off potential, 1.2 V (see FIG. 15). On the subsequent

discharge, the electrode does not show the characteristic plateau at 400 mV, but rather shows a continuous decrease in voltage to 0V.

The relatively poor performance of Li_2CuSn electrodes compared to Cu_6Sn_5 electrodes observed in these initial tests is attributed to the high reactivity of the Li_2CuSn phase (particularly in moist air), and to the difficulty of assembling Li_2CuSn electrodes and cells without some degradation of the electrode. From this viewpoint, it is clearly advantageous to load cells with unlithiated electrodes, such as Cu_6Sn_5 rather than with Li_2CuSn electrodes.

The addition of copper to a tin electrode decreases the theoretical capacity of the tin electrode, whereas increasing the tin content increases the capacity, see Table 3; Table 3 gives the theoretical capacity of Li_2CuSn in terms of its ideal fully-delithiated composition CuSn; it has the same composition as Cu_6Sn_6 ($\delta=1$). Complete removal of lithium from Li_2CuSn corresponds to a capacity of 273 mAh/g. Compared to the theoretical capacity of 372 mAh/g for LiC_6, the gravimetric capacity of the copper-tin electrodes, when lithiated to a 1:1 Li:Sn ratio is too small for it to be of practical interest for lithium-ion cells. However, for compositions reaching higher lithium content (for example, Li_7Sn_3 to $Li_{4.4}Sn$), the available capacity becomes more attractive, see Table 3. Note that in $Li_{13}Cu_6Sn_5$, which is believed to represent the maximum uptake of Li by the ideal η-Cu_6Sn_5, structure, the Li:Sn ratio is 2.6:1 which is close to that in Li_7Sn_3 (2.3:1). Because lithium-metal alloy systems have high crystallographic densities, they provide significantly higher volumetric capacities than lithiated carbon, LiC_6 (~750 mAh/ml). For example, Cu_6Sn_5 has a density of 8.28 g/ml; it will, therefore, provide a volumetric capacity of approximately 2450 mAh/ml when discharged to a Li_7Sn_3 composition ($Li_{11.67}Cu_6Sn_5$). A major advantage of these intermnetallic electrodes, therefore, is that they will occupy less volume than lithiated carbon electrodes for a given capacity value.

The capacity vs. cycle no. for Li/Sn and $Li/Cu_6Sn_{5+\delta}$ ($\delta=0, +1, -1, -3$) and Li/Li_2CuSn cells cycled over the range 1.2 to 0 V for the first 20 cycles is shown in FIG. 16. Although a pure tin electrode provides a significantly higher capacity on the initial discharge (~670 mAh/g) than copper-tin electrodes, the capacity of the pure tin electrodes decreases rapidly on cycling, dropping to ~115 mAh/g after 10 cycles. By contrast, the copper-tin electrodes $Cu_6Sn_{5+\delta}$ ($\delta=0, +1, -1, -3$) show lower capacity, but significantly better stability to electrochemical cycling. Cu_6Sn_6, Cu_6Sn_5, and Cu_6Sn_4 electrode powders that were not subjected to high-energy ball milling deliver 350,340 and 440 mAh/g on the initial discharge, and 180, 175 and 280 mAh/g after 10 cycles, respectively. The copper-rich electrodes Cu_6Sn_4 ($\delta=-1$) and Cu_6Sn_2($\delta=-3$) show the greatest cycling stability after 20 cycles, in agreement with the hypothesis that higher concentrations of inactive component in composite copper-tin electrodes should enhance electrochemical recharge ability. Reducing the voltage window to 1.2 to 0.2 V improves the cycling stability of the copper-tin electrodes even further; in this case, excellent cycling stability is achieved but at the expense of some capacity. For example, over this voltage range, the $Cu_6 Sn_4$ electrode delivers an initial capacity of 165 mAh/g, which increases on cycling as the electrode is "conditioned"; it delivers a steady 190 mAh/g after 10 cycles, see FIG. 17. This extra stability is attributed to two major factors: 1) the reversible topotactic reaction of lithium into the Cu_6Sn_5 component, and 2) to the presence of an inactive, electronically copper component that serves to counter the deleterious volumetric expansion/contraction

11

12

of any binary Li_xSn alloys that might be formed during cycling, particularly towards the end of discharge when the lithium concentration at the copper-tin intermetallic surface exceeds the limit allowed by the topotactic lithium insertion reaction, i.e., in excess of the lithium content in $Li_{-13}Cu_6Sn_5$.

A further example of the stability of the internetallic insertion electrodes of the present invention is given with respect to the compound InSb with a zinc-blende-type structure.

FIG. **20***a* shows the X-ray diffraction pattern of an initial InSb electrode having the zinc-blende-type structure. FIGS. **20***b* and **20***c* show the patterns of a Li_xInSb electrode after the initial electrochemical lithiation of a Li/inSb cell to a 0.5 volt and subsequent delithiation reaction to 1.2 volt, respectively. The X-ray diffraction pattern of the Li_xInSb electrode at 0.5 volt (FIG. **20***b*) resembles that of the parent InSb structure (FIG. **20***a*) but has a cubic lattice parameter 6.553 Å which is slightly larger than that of InSb (6.475 Å), as reflected by the slight shift of the peaks to lower two-theta values. This change in lattice parameter reflects only a small change in the cubic unit cell volume, namely, 3.66%. It is important to note that the X-ray diffraction pattern of the lithiated product in FIG. **20***b* also closely resembles that of Li_3Sb, because the idea structure of LI_3Sb can be regarded as a lithiated Li_2lnSb structure in which the In atoms have been replaced by Li. This finding has important implications for designing zinc-blende-type intermetallic insertion electrodes that are tolerant to at least some over lithiation of the structure. Furthermore, it is clear from the X-ray diffraction pattern in FIG. **20***c* that the zinc-blende-type structure of InSb is regenerated after subsequent lithium extraction to 1.2 volt.

The voltage profiles of the first 18 cycles of a Li/InSb cell and the capacity vs. cycle number plot for the first 22 cycles are shown in FIGS. **21** and **22**, respectively. It can be seen from FIGS. **21** and **22** that, apart from the first lithiation reaction, the electrochemical reaction is reversible when cells are cycled between 1.2 and 0.5 V. The exact reasons for the initial capacity loss on the first two cycles (450 to 290 mhAg, 64%) are unknown, although it can be speculated that this may be due to surface oxidation of the intermetallic electrode materials during processing. It is believed that this capacity loss can be reduced by improved processing techniques under inert conditions. Furthermore, in order to combat this capacity loss, the invention also includes intermetallic electrodes with additional lithium in the starting electrode, either as free lithium metal, or lithium as an integral part of the intermetallic electrode structure to compensate for any lithium that may be irreversibly locked within the negative intermetallic electrode during the initial lithiation reaction (charge) of the electrochemical cell.

Of particular significance to this invention is the typical profile of the Li/InSb cell shown in FIG. **23**. The theoretical capacity of the InSb electrode, when lithiated to the fliily lithiated zinc-blende composition Li_2InSb, is 229 mAh/g. Lithium insertion into InSb to form Li_2InSb is consistent with the two-stage reaction process that occurs between approximately 900 mV and 650 mV vs. Li in the expanded plot of cycle 10 in FIG. **24** because the two lithium atoms in the Li_2InSb are located in two crystallographically independent positions and hence have different site energies. Therefore, the data in FIGS. **21**, **22** and **23**, that show a reversible capacity between 290 and 250 mAh/g during at least the first twelve cycles, imply that InSb can be lithiated beyond the fially lithiated zinc-blende composition without severely damaging the reversibility of the cell or the InSb

zinc-blende structure that is generated after delithiation of the electrode at 1.2 volts vs. Li. Although the reasons for this excellent and surprising behavior have not precisely been determined, the X-ray diffraction data in FIGS. **20***a, b* and *c* suggests that further lithiation of Li_2InSb results in Li_3Sb-type structure which has a strong crystallographic relationship to both InSb and Li_2InSb-type structures. Such a reaction, which is believed to occur as a displacement reaction, can be represented (for complete reaction with lithium):

$$Li+Li_2InSb \leftrightarrows Li_3Sb_{1-x}In_x + x\ Sb + (1-x)In$$
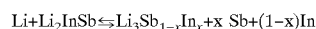
Because of the strong resemblance of the X-ray diffraction pattern in FIG. **20***b* in Li_3Sb, it is believed that the value of x in the reaction above is close or equal to zero and that In is preferentially extruded from the lattice in very finely divided form; the In can be reincorporated into the structure on reversing the direction of the current. The fact that all components of this system remain metallic or semiconducting at all states of charge and discharge is believed to contribute towards the good reversibility of the reaction, as well as the strong crystallographic relationship between the InSb, Li_2InSb and Li_3Sb intermetallic structures. The lithiation of InSb is analogous to that which occurs in some metal oxides at room temperature such as Fe_3O_4

$$Li+Fe_3O_4 \rightarrow LiFe_3O_4 + 7Li \rightarrow 4Li_2O + 3Fe$$
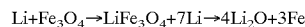
In contrast to the Li_xInSb intermetallic system, the lithiation of Fe_3O_4 at room temperature is irreversible, because of the nature of the Fe_3O_4 (spinel) to rocksalt ($LiFe_3O_4$) transformation and the insulating properties of the fully discharged Li_2O product. The overall reaction becomes more reversible at higher temperatures when iron can be more easily reincorporated back into the close-packed oxygen array to regenerate lithium-iron oxide spinel phases.

This invention is thus extended to include overlithiated intermetallic zinc-blende electrode structures, and particularly those with a Li_3Sb-type structure. Furthermore, an additional advantage of the Li_3Sb-type structure is that it can be used as an excellent end-of-charge indicator to signal full lithiation of the Li_2InSb-zinc-blende-type electrode structures.

As further examples to illustrate the scope of the invention as previously described herein, the copper atoms of the Cu_6Sn_5 NiAs-type) structure were partially replaced by Zn or Ni atoms, thus increasing and reducing the number of valence electrons associated with the metal elements in the structure, respectively. For example, the compounds $Cu_{6-x}Zn_xSn_5$ and $Cu_{6-y}Ni_ySn_5$ with x=1 and y=1 and y=2 were prepared, the X-ray diffraction patterns of which are illustrated in FIG. **24** showed that they were isostructural with Cu_6Sn_5. These compounds showed enhanced electrochemical behavior to Cu_6Sn_5. For example, FIG. **25** shows the typical charge/discharge profiles for cycles 4 to 7 of a $Li/Cu_{6-x}Zn_xSn_5$ cell when cycled between 1.2 and 0.2 V. A plot of capacity vs. cycle life for a $Li/Cu_{6-x}Zn_xSn_5$ cell and a $Li/Cu_{6-y}Ni_ySn_5$ (y=1) cell is shown in FIG. **26** where the dot (·) is Zn, and the star (*) is Ni. These samples were prepared in the presence of 3–5 w/o (weight percent) carbon, thereby allowing for the substitution of carbon atom for some of the metal atoms. If other non-metals were substituted for carbon, then these non-metals would also substitute for some of the metal atoms.

Therefore, in a further embodiment of the invention, it stands to reason that selective substitution of metal atoms with other atoms in the intermetallic host structure, such as

13

a NiAs-type structure, a NiIn-type structure and a zinc-blende type structure can be achieved without significantly altering their structures or seriously affecting the electrochemical performance of the electrode. Moreover, it is well known in the art that zinc-blende structures exist that are comprised of a metal atom and a non-metal atom, well known examples being the mineral zinc-blende itself, ZnS, and also AgO, GaP, and ZnSe, that contain the non-metal elements S, O, P and Se, respectively. Therefore, the invention also includes those intermetallic compounds defined above in which the metal atoms can be at least partially substituted by a non-metal element, the intermetallic compound preferably containing less than 50 atom percent of a non-metal element, more preferably less than 20 atom percent of a non-metal element, and most preferably less than 10 atom percent of a non-metal element, the non-metals being selected from one or more of B, C, N, O, F, P, S, Cl, As, Se, Br, Te and I.

This invention thus also embodies electrode intermetallic host structures that transform on lithiation to a lithiated zinc-blende-type structure in the presence of an additional substantially inactive (non-alloying) element (or elements) with respect to lithium, or alternatively, an additional substantially active alloying element (or elements) with respect to lithium, or both.

In this regard, the invention also encompasses the use of carbonaceous additives, such as graphite and pyrolyzed carbons, to the intermetallic negative electrode, thereby providing a composite electrode structure or composite matrix to improve the current collection around electronically disconnected particles. Additional advantages of carbonaceous additives are that they can also contribute to the overall electrochemical capacity of the negative electrode and to provide end-of-charge indicators to prevent over-lithiation of the intermetallic electrode materials.

EXPERIMENTAL

Example 1

Cu_6Sn_5 was synthesized by reacting metallic tin and metallic copper in stoichiometric amounts at 400° C. under argon for 12 hours. The sample was ground by mechanical milling to an average particle size of less than 10 microns. X-ray diffraction data, collected on a Siemens D5000 powder diffractometer with CuKα radiation showed that the Cu_6Sn_5 product was an essentially single-phase product as shown in FIG. **7**a.

Example 2

Copper-rich and tin-rich materials $Cu_6Sn_{5+\delta}$ ($\delta=1$, -3), i.e., Cu_6Sn_6, Cu_6Sn_4, and Cu_6Sn_2 were prepared in identical fashion to Cu_6Sn_5 in Example 1 with the required excess/deficiency of copper. The samples were ground by mechanical milling to an average particle size of less than 10 microns. The copper-rich and tin-rich materials showed the characteristic peaks of Cu_6Sn_5 and additional peaks of copper and tin metal, respectively.

Example 3

Li_2CuSn was prepared by heating lithium metal, copper metal and tin metal at 900° C. under argon for 3 hours. The sample was ground by mechanical milling to an average particle size of less than 40 microns. X-ray diffraction data, collected on a Siemens D5000 powder diffractometer with CuKα radiation showed that the Li_2CuSn product was an essentially singlephase product as shown in FIG. **7**c.

14

Example 4

Li_2CuSn was chemically delithiated by reaction with $NOBF_4$ in acetonitrile at room temperature. X-ray diffraction data, collected on a Siemens D5000 powder diffractometer with CuKα radiation showed that the product was an essentially single-phase product with a Cu_6Sn_5-type structure as shown in FIG. **7**d.

Example 5

Ni_3Sn_2 was synthesized by reacting metallic tin and metallic nickel in stoichiometric amounts at 650° C. under argon for 12 hours. The sample was ground by mechanical milling to an average particle size of less than 40 microns. X-ray diffraction data, collected on a Siemens D5000 powder diffractometer with CuKα radiation showed that the Ni_3Sn_2 product was an essentially single-phase product as shown in FIG. **18**.

Example 6

Li_2AgSn was prepared by heating lithium metal; silver metal and tin metal at 900° C. under argon for 3 hours. The sample was ground by mechanical milling to an average particle size of less than 40 microns. X-ray diffraction data, collected on a Siemens D5000 powder diffractometer with CuKα radiation showed that the Li_2AgSn product was an essentially single-phase product as shown in FIG. **19**.

Example 7

InSb was prepared by ball-milling indium metal and antimony metal powder at room temperature in air for 20 hours. Thereafter, the sample was annealed under argon for 10 hours at 400° C., and subsequently ground to an average particle size of less than 40 microns. X-ray diffraction data, collected on a Siemens D5000 powder diffractometer with CuKα radiation showed that the InSb product was an essentially single-phase product as shown in FIG. **20**a.

Example 8

Samples of $Cu_{6-x}Zn_xSn_5$ were prepared by ball milling Cu, Zn, and Sn in the appropriate stoichiometric ratios with values between 0<x<6. For these samples, 3–5% weight percent (about 25 atom percent) carbon was added as a solid lubricant into the mixer. Samples were examined by powder XRD using a Siemens D5000 powder diffractometer with CuKα radiation. The samples were found to be single phase in the range of (0<x<2). The X-ray pattern showing the single phase product Cu_5ZnSn_5 (x=1) is shown in FIG. **24**.

Example 9

Samples of $Cu_{6-y}Ni_ySn_5$ were prepared by ball milling Cu, Ni and Sn in the appropriate stoichiometric ratios with values between 0<y<6. For these samples, 3–5% weight percent (about 25 atom percent) carbon was added as a solid lubricant into the mixer. Samples were examined by powder XRD using a Siemens D5000 powder diffractometer with CuKα radiation. The samples were found to be single phase in the range of (0<y<3). The X-ray patterns showing the single phase products Cu_5NiSn_5 (y=1) and $Cu_4Ni_2Sn_5$ (y=2) are shown in FIG. **24**.

Example 10

The intermetallic materials were evaluated as electrodes in coin cells (size 1225) 12 mm diameter and 2.5 mm high against a counter lithium electrode. The cells had the con-

figuration: Li/1M LiPF$_6$ in ethylene carbonate, diethyl carbonate (50:50)/Intermetallic electrode. For the intermetallic electrodes, laminates were made containing approximately 6 mg (81%) of the intermetallic compound, intimately mixed with 10% (by weight) binder (Kynar 2801) and 9% (by weight) carbon (XC-72) in tetrahydrofuran (THF). Metallic lithium foil was used as the counter (negative) electrode. Li/Copper-tin cells were charged and discharged at constant current (generally at 0.1 mA), within the voltage range of either 1.2 to 0.0 V, or 1.2 to 0.2 V and Li/InSb cells within the voltage range of 1.2 to 0.5 volts. The electrochemical data from the various intermetallic electrodes are shown in various electrochemical plots, as in FIG. **10**: a Li/Cu$_6$Sn$_5$ cell; FIG. **11**: a Li/Sn cell (reference); FIG. **12**: a Li/Cu$_6$Sn$_6$ cell, FIG. **13**; a Li/Cu$_6$Sn$_5$ cell; FIG. **14**: a Li/Cu$_6$Sn$_4$ cell; FIG. **15**: a Li/Li$_2$CuSn cell; FIG. **16**: a collective plot of Li/Sn, Li/Cu$_6$Sn$_6$, Li/Cu$_6$Sn$_5$, Li/Cu$_6$Sn$_4$, Li/Cu$_6$Sn$_2$ and Li/Li$_2$CuSn cells; FIG. **17**: a second collective plot of Li/Sn, Li/Cu$_6$Sn$_6$, Li/Cu$_6$Sn$_5$ and Li/Cu$_6$Sn$_4$ cells; FIG. **21**: a Li/InSb cell; and FIG. **22**: a Li/InSb cell. FIG. **23**, a Li/SnSb cell, FIG. **25**, a Li/Cu$_{6-x}$Zn$_x$Sn$_5$ (x=1) cell, and FIG. **26**, a Li/Cu$_{6-x}$Zn$_x$Sn$_5$ (x=1) and a Li/Cu$_{6-y}$Ni$_y$Sn$_5$ (y=1) cell.

TABLE 1

A comparison of the theoretical gravimetric and volumetric capacities of various negative electrode (anode) materials based on Cu$_6$Sn$_5$ and Li$_2$CuSn-type materials with Li$_x$C$_6$. Volumetric capacities are calculated using the approximate density of the delithiated electrodes

	Li$_x$C$_6$	η-Li$_x$ Cu$_6$Sn$_5$	η'-Li$_x$ Cu$_6$Sn$_5$	Li$_x$Ni$_3$Sn$_2$	Li$_x$Co$_3$Sn$_2$	Li$_x$MgSi
X$_{max}$	1	13	9	3	3	2
Th. Gr. Cap. (mAh/g)	372	358	248	195	194	1023
Approx. density of delithiated electrode (g/ml)	2.2	7.0	8.3	9.0	9.0	2.2
Th. Vol. Cap. (mAh/ml)	818	2506	2058	1755	1746	2251

TABLE 2

A list of examples of materials with a lithiated zinc-blende-type structure where the sum of the non lithium atoms equals 2 in a Li$_2$AB structure and A and B are non-lithium atoms.

Li$_2$Ag$_x$Bi$_{2-x}$	Li$_2$Ag$_x$Pb$_{2-x}$	Li$_2$Ag$_x$Sb$_{2-x}$	Li$_2$AgSn
Li$_2$AuBi	Li$_2$AuGa$_x$	Li$_2$AuGe	Li$_2$Au$_x$In$_{2-x}$
Li$_2$AuPb	Li$_2$Au$_x$Sb$_{2-x}$	Li$_2$AuSn	—
Li$_2$CdPb	Li$_2$CdSn	Li$_2$CuSb	Li$_2$CuSn
Li$_2$GeSn	Li$_2$IrAl	Li$_2$IrGa	Li$_2$IrIn
Li$_2$Mg$_x$In	—	—	—
Li$_2$MgSi	Li$_2$PdSb	Li$_2$PdGa	Li$_2$PdIn
Li$_2$PdPb	Li$_2$PdSb	Li$_2$PtAl	Li$_2$PtGa
Li$_2$PtIn	Li$_2$PtSb	Li$_2$RhAl	Li$_2$RhGa
Li$_2$RhIn	Li$_2$Zn$_x$Cd$_{2-x}$	Li$_{8.96}$Zn$_{3.20}$Pb$_{3.84}$	
	Li$_2$ZnSb		

Crystallographic Parameters for Li$_2$CuSn

Space Group: F – 43 m; a = 6.27 Å

Atom	Wyckoff Site	x	y	z	Occupancy (%)
Li1	4(b)	0.5	0.5	0.5	100
Li2	4(c)	0.25	0.25	0.25	100

TABLE 2-continued

A list of examples of materials with a lithiated zinc-blende-type structure where the sum of the non lithium atoms equals 2 in a Li$_2$AB structure and A and B are non-lithium atoms.

Cu	4(d)	0.75	0.75	0.75	100
Sn	4(a)	0	0	0	100

TABLE 3

Relative Capacities of Sn, CuSn, and Cu$_6$Sn$_{5+\delta}$ (δ = 0, ±1)

Electrode	δ in Cu$_6$Sn$_{5+\delta}$	Theor. Capacity* (mAh/g) to LiSn composition	Theor. Capacity* (mAh/g) to Li$_7$Sn$_3$ composition	Theor. Capacity* (mAh/g) to Li$_{4.4}$Sn composition
Sn	–	226	527	994
CuSn (from Li$_2$CuSn)	(+1)	147	343	647
Cu$_6$Sn$_4$	–1	125	292	551
Cu$_6$Sn$_5$	0	137	320	604
Cu$_6$Sn$_6$	+1	147	343	647

*Based on mass of starting electrode

Intermetallic electrodes based on the Cu$_6$Sn$_5$ and Li$_2$CuSn structure types have been discovered to be usefuil negative electrodes for lithium-ion cells. The new anodes that operate substantially by a topotactic reaction mechanism may provide a significant improvement over the cycling capability of state-of-the-art binary lithium alloy electrodes. Cycling stability of these electrodes is however, gained at the expense of the capacity of the binary lithium alloy systems.

While there has been disclosed what is considered to be the preferred embodiment of the present invention, it is understood that various changes in the details may be made without departing from the spirit, or sacrificing any of the advantages of the present invention.

The embodiments of the invention in which an exclusive property or privilege is claimed are defined as follows:

1. A negative electrode for a non-aqueous electrochemical cell of an intermetallic host structure containing two or more elements selected from the metal elements and silicon, having a hexagonally-close packed NiAs-type structure or a defect-Ni$_2$In-type structure capable of accommodating lithium within its crystallographic host structure such that when lithiated it transforms to a cubic-close-packed structure.

2. The negative electrode of claim **1**, wherein the metal atoms are at least partially disordered in the NiAs-type and defect —Ni$_2$In-type structures.

3. The negative electrode of claim **1**, wherein the host intermetallic compound is one or more of Cu$_6$Sn$_5$, Cu$_6$Sn$_5$ in which the Cu ions are partially substituted by Zn and/or Ni.

4. The negative electrode of claim **1**, wherein the host intermetallic structure includes two or more elements selected from Sn, Si, Al, Ga, Ge, In, Pb, Zn, Cd, Hg, Sb, Cu, Ni, Co, Fe, Mn, Cr, V, Ti, Mg, Ca and Ag.

5. The negative electrode of claim **1**, wherein the host intermetallic structure contains additional lithium as free lithium metal or as an integral part of the intermetallic structure.

6. The negative electrode of claim **1**, which when overlithiated, a Li$_3$Sb-related structure is present in the negative electrode.

7. The negative electrode of claim **1**, wherein carbon is present in a composite matrix.

8. The negative electrode of claim **7**, wherein graphite is present in the composite matrix.

9. The negative electrode of claim **4**, wherein the host intermetallic structure includes two or more elements selected from Sn, Si, Al, Ga, Zn, Cu, Ni, Co, and Mg.

10. The negative electrode of claim **1**, wherein the metal atoms and lithium atoms are at least partially disordered in the cubic-close-packed structures.

11. The negative electrode of claim **1**, wherein the cubic-close-packed structure is Li_2CuSn.

12. The negative electrode of claim **1**, wherein the cubic-close-packed structure is Li_2CuSn.

13. The negative electrode of claim **1**, wherein the cubic-close-packed structure is Li_2MgSi.

14. The negative electrode of claim **1**, wherein the intermetallic host structure is particulate having an average particle size of less than about 40 microns.

15. The negative electrode of claim **1**, wherein the intermetallic host structure transforms on lithiation to a cubic-close-packed structure in the presence of an additional, substantially active alloying element or elements with respect to lithium or substantially inactive non-alloying element or elements with respect to lithium or both.

16. The negative electrode of claim **1**, wherein the metal atoms of the intermetallic host structure are partially substituted by less than 50 atom percent of a non-metal selected from B, C, N, O, F, P, S, Cl, As, Se, Br, Te and I.

17. The negative electrode of claim **1**, wherein the metal atoms of the intermetallic host structure are partially substituted by less than 20 atom percent of a non-metal.

18. The negative electrode of claim **17**, wherein the metal atoms of the intermetallic host structure are partially substituted by less than 10 atom percent of a non-metal.

19. A negative electrode for a non-aqueous electrochemical cell consisting of an intermetallic host structure containing two or more elements selected from Sn, Si, Al, Ga, Ge, In, Pb, Zn, Cd, Hg, Sb, Cu, Ni, Co, Fe, Mn, Cr, V, Ti, Mg, Ca and Ag, capable of accommodating lithium within its crystallographic host structure such that when lithiated it transforms by a substantially topotactic phase transition mechanism to a cubic-close-packed structure.

20. A non-aqueous electrochemical cell comprising a negative electrode, an electrolyte and a positive electrode, the negative electrode consisting of an intermetallic host structure containing two or more elements selected from the metal elements and silicon, having a hexagonally-close-packed NiAs-type structure or a defect-Ni_2In type structure capable of accommodating lithium within its crystallographic host structure such that when lithiated it transforms to a cubic-close-packed structure.

21. The non-aqueous electrochemical cell of claim **20**, wherein the host intermetallic structure includes two or more elements selected from Sn, Si, Al, Ga, Ge, In, Pb, Zn, Cd, Hg, Sb, Cu, Ni, Co, Fe, Mn, Cr, V, Ti, Mg, Ca and Ag.

22. The non-aqueous electrochemical cell of claim **20**, wherein the cubicclose-packed type structure of the negative electrode is Li_2CuSn.

23. The non-aqueous electrochemical cell of claim **21**, wherein the cubic close-packed type structure of the negative electrode is derived from Cu_6Sn_5.

24. A method of making an electrochemical cell comprising providing a negative electrode, providing an electrolyte and providing a positive electrode, the negative electrode consisting of an intermetallic host structure containing two or more elements selected from the metal elements and

silicon, having a hexagonally-closepacked NiAs-type structure or a defect-Ni_2In-type structure capable of accommodating lithium within its crystallographic host structure such that when lithiated it transforms to a cubic-close-packed type structure and assembling the electrodes and electrolyte into an electrochemical cell.

25. The method of claim **24**, wherein the electrochemical cell is assembled in its discharged state with substantially no lithium in the negative anode.

26. The method of claim **24**, wherein the electrochemical cell is assembled in its charged or partially charged state with lithium in the negative electrode.

27. The method of claim **24**, wherein the electrochemical cell contains additional lithium as free lithium metal or as integral part of intermetallic electrode structure.

28. The method of claim **24**, wherein the electrochemical cell contains a negative electrode which can be overlithiated to provide additional capacity or a voltage indicator to signal the end-of-charge in the electrochemical cell.

29. A non-aqueous battery comprising a plurality of cells electrically connected, each cell comprising a negative electrode, an electrolyte and a positive electrode, the negative electrode consisting of an intermetallic host structure containing two or more elements selected from the metal elements and silicon, having a hexagonally-close-packed NiAs-type structure or a defect-Ni_2In-type structure capable of accommodating lithium within its crystallographic host structure such that when lithiated it transforms to a cubic-close-packed type structure.

30. A negative electrode for a non-aqueous electrochemical cell of an intermetallic host structure containing two or more elements selected from the metal elements and silicon, with a NiAs or defect—Ni_2In type structure, capable of accommodating lithium within its crystallographic host structure such that when lithiated it transforms to a lithiated NiAs-type structure.

31. The negative electrode of claim **30**, wherein there is additional lithium present as free lithium or as an integral part of the intermetallic electrode structure.

32. The negative electrode of claim **30**, which when overlithiated, a Li_3Sb-type structure is present in the negative electrode.

33. The negative electrode of claim **30**, wherein carbon is present in a composite matrix.

34. The negative electrode of claim **30**, wherein graphite is present in a composite matrix.

35. A method of making an electrochemical cell comprising providing a negative electrode, providing an electrolyte and providing a positive electrode, the negative electrode consisting of an intermetallic host structure containing two or more elements selected from the metal elements and silicon, with a NiAs or defect—Ni_2In-type structure, capable of accommodating lithium within its crystallographic host structure such that when lithiated it transforms to a lithiated NiAs-type structure, and assembling the electrodes and electrolyte to form an electrochemical cell.

36. The method of claim **35**, wherein the electrochemical cell is assembled in its discharged state with substantially no lithium in the negative anode.

37. The method of claim **35**, wherein the electrochemical cell is assembled in its charged or partially charged state with lithium in the negative electrode.

38. The method of claim **33**, wherein the electrochemical cell contains additional lithium as free lithium metal or as an integral part of an intermetallic electrode structure.

39. The method of claim **35**, wherein the electrochemical cell contains a negative electrode which can be overlithiated

to provide additional capacity or a voltage indicator to signal the end-of-charge in the electrochemical cell.

40. A non-aqueous battery comprising a plurality of cells electrically connected, each cell comprising a negative electrode, an electrolyte and a positive electrode, the negative electrode consisting of an intermetallic host structure containing two or more elements selected from the metal elements and silicon with a NiAs or defect—Ni_2In-type

structure, capable of accommodating lithium within its crystallographic host structure such that when lithiated it transforms to a lithiated NiAs-type structure.

41. The non-aqueous battery of claim **40**, which when the negative electrode is overlithiated, a Li_3Sb-type structure is present in the negative electrode.

*   *   *   *   *